New Complexes of Chromium(III) Containing Organic π-Radical Ligands: An Experimental and Density Functional Theory Study

ARTICLE *in* INORGANIC CHEMISTRY · MARCH 2013

Impact Factor: 4.76 · DOI: 10.1021/ic302743s · Source: PubMed

Inorganic Chemistry

Article

pubs.acs.org/IC

New Complexes of Chromium(III) Containing Organic π-Radical Ligands: An Experimental and Density Functional Theory Study

Mei Wang,[†,¶] Jason England,[†,¶] Thomas Weyhermüller,[†] Swarna-Latha Kokatam,[†] Christopher J. Pollock,[†] Serena DeBeer,[†,§] Jingmei Shen,[‡] Glenn P.A. Yap,[‡] Klaus H. Theopold,[‡] and Karl Wieghardt*[,†]

[†]Max-Planck-Institut für Chemische Energiekonversion, Stiftstrasse 34-36, D-45470 Mülheim an der Ruhr, Germany

[§]Department of Chemistry and Chemical Biology, Baker Laboratory, Cornell University, Ithaca, New York 14853, United States

[‡]Department of Chemistry and Biochemistry, University of Delaware, Newark, Delaware 19716, United States

Supporting Information

ABSTRACT: The electronic structures of a series of chromium complexes **1**−**7** have been experimentally investigated using a combination of X-ray crystallography, magneto- and electrochemistry, and Cr K-edge X-ray absorption and UV−vis spectroscopies. Reaction of the dimer $[Cr^{II}_2(\mu\text{-}CH_3CO_2)_4]^0$ with 2,2′-bipyridine (bpy^0) produced the complex $[Cr^{III}(bpy^0)(bpy^{\bullet})(CH_3CO_2)_2]^0$ ($S = 1$) (**1**), but in the presence of isopropylamine ($^iPrNH_2$) $[Cr^{III}(bpy^{\bullet})(^iPrNH_2)_2(CH_3CO_2)_2]^0$ ($S = 1$) (**2**) was obtained. Both **1** and **2** contain a Cr^{III} ion and a single $(bpy^{\bullet})^{1-}$ ligand, so are *not* low-spin Cr^{II} species. One-electron oxidation of **1** and **2** yielded $[Cr^{III}(bpy^0)_2(CH_3CO_2)_2]PF_6$ ($S = 3/2$) (**3**) in both cases. In addition, the new neutral species $[Cr^{III}(DAD^{\bullet})_3]^0$ ($S = 0$) (**4**) and $[Cr^{III}(CF_3AP^{\bullet})_3]^0$ ($S = 0$) (**5**) have been synthesized. Both complexes contain three π-radical anion ligands, which derive from one electron reduction of 1,4-bis(cyclohexyl)-1,4-diaza-1,3-butadiene and one electron oxidation of 2-(2-trifluoromethyl)-anilino-4,6-di-*tert*-butylphenolate, respectively. Intramolecular antiferromagnetic coupling to d^3 Cr^{III} gives the observed singlet ground states. Reaction of $[Cr^{II}(CH_3CN)_6](PF_6)_2$ with 2,6-bis[1-(4-methoxyphenylimino)ethyl]pyridine (PDI^0) under anaerobic conditions affords dark brown microcrystals of $[Cr^{III}(PDI^0)(PDI^{\bullet})](PF_6)_2$ ($S = 1$) (**6**). This complex is shown to be a member of the electron transfer series $[Cr^{III}(PDI)_2]^{3+/2+/1+/0}$, in which all one-electron transfer processes are ligand-based. By X-ray crystallography, it was shown that **6** possesses a localized electronic structure, such that one ligand is neutral (PDI^0) and the other is a π-radical monoanion $(PDI^{\bullet})^{1-}$. Again, it should be highlighted that **6** is *not* a Cr^{II} species. Lastly, the structure of $[Cr^{III}(^{Me}bpy^{\bullet})_3]^0$ ($S = 0$) (**7**, ^{Me}bpy = 4,4′-dimethyl-2,2′-bipyridine) has been established by high resolution X-ray crystallography and clearly shows that three $(^{Me}bpy^{\bullet})^{1-}$ radical anions are present. To further validate our electronic structure assignments, complexes **1**−**6** were investigated computationally using density functional theory (DFT) and found in all cases to contain a Cr^{III} ion. This oxidation state assignment was experimentally confirmed for complexes **2**, **4**, **5**, and **6** by Cr K-edge X-ray absorption spectroscopy.

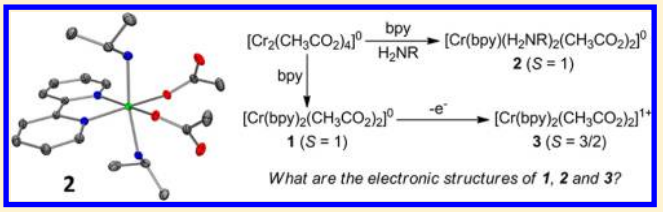

INTRODUCTION

Over the past few decades, ligand noninnocence has gone from being of marginal concern to a subject of intense research.[1] This transformation was in large part due to recognition of its importance in enzymatic systems and potential utility in catalysis. However, it also served to highlight that a formal oxidation state is not necessarily the same as a spectroscopic oxidation state.[2] Furthermore, recognition of ligand noninnocence does not always equate to an ability to correctly assign electronic structure. This is achieved on a case-to-case basis by use of a combination of comprehensive spectroscopic studies and density functional theory (DFT) calculations, which is very labor intensive. Hence, it is clear the development of predictive correlations would be of great help, but this would require access to large quantities of empirical data. The literature already contains large numbers of complexes of potentially noninnocent ligands and, although many may have been recognized as such, accurate electronic structure assignment is lacking in many cases.

Our recent efforts to rectify this situation have centered of the coordination chemistry of 2,2′-bipyridine (bpy) and 2,2′,6′,2″-terpyridine (terpy).[3] Chromium complexes of these ligands have proved particularly useful in this regard due to the minimal covalency of their bonding and the high stability of the high-spin Cr^{III} ion, which has allowed in-depth characterization of the redox properties of these ligands in the absence of other complicating factors. Indeed, we recently demonstrated that a series of textbook low-spin Cr^{II} bpy complexes actually contain Cr^{III} antiferromagnetically coupled to a $(bpy^{\bullet})^{1-}$ π-radical anion.[3f] However, these findings do not exclude the possibility of bpy complexes with Cr oxidation states less than +III, such

Received: December 13, 2012
Published: March 26, 2013

as the genuine Cr^{II} complexes of (bpy^0) and $(bpy^{\bullet})^{1-}$ recently detailed by Goicoechea and co-workers.[4] In these complexes, the high-spin d^4 electron configuration is stabilized by a square planar geometry. In pursuit of a deeper understanding of these complex systems, the studies detailed herein further expand the range of electronically well-characterized Cr complexes of redox noninnocent ligands available for analysis.

In 1963, Herzog et al. reported that reaction of the dinuclear complex $[Cr^{II}_2(\mu\text{-}CH_3CO_2)_4]^0{\cdot}2THF$ (THF = tetrahydrofuran) with 4 equivalents of (bpy^0) in THF produces an air sensitive black powder corresponding to mononuclear $[Cr(bpy)_2(CH_3CO_2)_2]^0$ (**1**, eq 1), which has a magnetic moment of 3.01 μ_B at ambient temperature in accord with a $S = 1$ ground state.[5,6] On this basis, the authors formulated **1** as a low-spin Cr^{II} complex. The presence of isopropylamine ($^iPrNH_2$) in the aforementioned reaction led to formation of a different air-sensitive complex, $[Cr(bpy)(^iPrNH_2)_2(CH_3CO_2)_2]^0$ (**2**, eq 2), which was also described as a low-spin Cr^{II} species with an $S = 1$ ground state.[5] Complex **2** can also be obtained by addition of $^iPrNH_2$ to solutions of **1** (eq 3).

$$[Cr^{II}_2(\mu\text{-}CH_3CO_2)_4]^0 + 4(bpy^0) \rightarrow 2[Cr^{II}(bpy^0)_2(CH_3CO_2)_2]^0 \quad (1)$$

$$[Cr^{II}_2(\mu\text{-}CH_3CO_2)_4]^0 + 4{}^iPrNH_2 + 2(bpy^0) \rightarrow 2[Cr^{II}(bpy^0)(^iPrNH_2)_2(CH_3CO_2)_2]^0 \quad (2)$$

$$[Cr(bpy)_2(CH_3CO_2)_2]^0 + 2{}^iPrNH_2 \rightarrow [Cr(bpy)(^iPrNH_2)_2(CH_3CO_2)_2]^0 + (bpy^0) \quad (3)$$

Herein, we also report the formation of $[Cr(bpy)_2(CH_3CO_2)_2](PF_6)$ ($S = 3/2$) (**3**) by one-electron oxidation of **1** using $AgPF_6$, and its characterization by spectroscopy and X-ray crystallography. The bpy structural parameters in **3** are typical of the neutral ligand and clearly distinct from those of the bpy ligand in the crystal structure of **2**, which are characteristic of a $(bpy^{\bullet})^{1-}$ radical anion. Hence, we are able to structurally distinguish between the $Cr^{III}(bpy^0)$ and $Cr^{III}(bpy^{\bullet})$ five-membered chelate rings. Similarly, in a recent publication,[3f] we demonstrated that the $S = 1$ complex $[Cr(^tbpy)_2Cl_2]^0$ is not a low-spin Cr^{II} species, as previously thought, but should be formulated as $[Cr^{III}(^tbpy^0)(^tbpy^{\bullet})Cl_2]^0$ containing a neutral ($^tbpy^0$) ligand and a π-radical anion $(^tbpy^{\bullet})^{1-}$ that is antiferromagnetically coupled to a Cr^{III} center. Remarkably, the differing oxidation states of the two bpy ligands in the complex were apparent by X-ray crystallography due to their distinct C−C and C−N bond distances. A similarly localized electronic structure was also observed in $[Cr^{III}(^tbpy^0)_2(^tbpy^{\bullet})](PF_6)_2$ ($S = 1$).[3b,7] These oxidation state assignments were confirmed by measuring the Cr K-pre-edge energy of these complexes by X-ray absorption spectroscopy (XAS), which allows one to unambiguously distinguish between Cr oxidation states of +II (high-spin and low-spin) and +III in an octahedral ligand environment.[3b,d]

Neutral octahedral complexes of chromium ligated by three bidentate ligands $[CrL_3]^0$ exhibit diamagnetic ($S = 0$) ground states, and in the past, they were often described as containing "low-valent" chromium (d^6 low-spin Cr^0) and three neutral ligands L^0. More recently, this electronic description has been revoked and a reformulation, based upon extensive spectroscopic (UV−vis, Cr K-edge XAS, magnetochemistry) and DFT studies, as Cr^{III} ions antiferromagnetically coupled to three π-radical anion ligands $[Cr^{III}(L^{\bullet})_3]^0$ has been forwarded. To date, the ligands investigated in this context include mononanionic semiquinones,[8] singly reduced 1,2-diketones,[9] bipyridine π-radical anions,[3b] and 1,2-dithiolene radical monoanions.[10] In this study, we add two new examples of neutral $[Cr^{III}(L^{\bullet})_3]^0$ complexes, **4** and **5** (Chart 1), which contain three 1,2-diimine radical anions and three *ortho*-iminobenzosemiquinone anions, respectively.

Chart 1. Ligand Abbreviations and Complexes

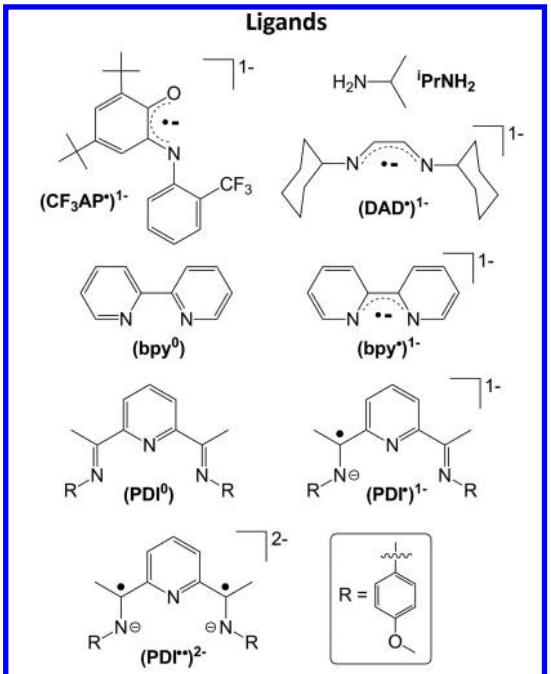

Complexes

$[Cr^{III}(bpy^0)(bpy^{\bullet})(CH_3CO_2)_2]^0$	**(1)**	($S = 1$)
$[Cr^{III}(bpy^{\bullet})(^iPrNH_2)_2(CH_3CO_2)_2]^0$	**(2)**	($S = 1$)
$[Cr^{III}(bpy^0)_2(CH_3CO_2)_2](PF_6)$	**(3)**	($S = 3/2$)
$[Cr^{III}(DAD^{\bullet})_3]^0$	**(4)**	($S = 0$)
$[Cr^{III}(CF_3AP^{\bullet})_3]^0$	**(5)**	($S = 0$)
$[Cr^{III}(PDI^0)(PDI^{\bullet})](PF_6)_2$	**(6)**	($S = 1$)
$[Cr^{III}(^{Me}bpy^{\bullet})_3]^0$	**(7)**	($S = 0$)

We have also synthesized $[Cr(PDI)_2]^{2+}$ (**6**, $S = 1$), where PDI represents a generic pyridine-2,6-diimine ligand and (PDI^0) and $(PDI^{\bullet})^{1-}$ are its neutral and radical anion forms (Chart 1), both of which are present in **6**. Hence, this complex is best formulated as $[Cr^{III}(PDI^0)(PDI^{\bullet})]^{2+}$ ($S = 1$). An analogous electronic structure has been reported for $[Cr^{III}(terpy^0)(terpy^{\bullet})]^{2+}$ ($S = 1$), where $(terpy^0)$ is neutral 2,2′,6′,2″-terpyridine and $(terpy^{\bullet})^{1-}$ is its anionic π-radical analog.[3d] Finally, we have synthesized and, for the first time, crystallographically characterized the *neutral* complex $[Cr^{III}(^{Me}bpy^{\bullet})_3]^0$ ($S = 0$, where ^{Me}bpy is 4,4′-dimethyl-2,2′-bipyridine) (**7**). This is an analog of $[Cr^{III}(^tbpy^{\bullet})_3]^0$ (^{t}bpy = 4,4′-di-*tert*-butyl-2,2′-bipyridine), a member of the electron transfer series $[Cr^{III}(^tbpy)_3]^n$ (n = 3+ to 3−), which we previously extensively characterized by spectroscopy and density functional theory (DFT) studies.[3b] However, we were

dx.doi.org/10.1021/ic302743s | Inorg. Chem. 2013, 52, 4472−4487

Table 1. Crystallographic Data for Complexes 1−7

	1	2	3	4	5	6·0.1 H_2O	7
chem. formula	$C_{24}H_{22}CrN_4O_4$	$C_{20}H_{32}CrN_4O_4$	$C_{24}H_{22}CrF_6N_4O_4P$	$C_{42}H_{72}CrN_6$	$C_{63}H_{72}CrF_9N_3O_3$	$C_{46}H_{46.22}CrF_{12}N_6O_{4.11}P_2$	$C_{36}H_{36}CrN_6$
fw	482.46	444.50	627.43	713.06	1142.24	1090.72	604.71
space group	*C*2/*c*, No. 15	$P2_1/n$, No. 14	$P2_1/n$, No. 14	*R*-3*c*, No. 167	$P2_1/c$, No. 14	$P2_1/c$, No. 14	*R*-3*c*, No. 167
a, Å	8.0904(11)	9.6230(12)	8.157(2)	17.205(2)	25.1758(6)	18.281(3)	18.1839(13)
b, Å	18.019(3)	16.838(2)	10.131(2)	17.205(2)	11.2059(2)	16.469(2)	18.1839(13)
c, Å	15.221(2)	14.639(2)	31.714(7)	46.944(8)	24.0098(4)	17.2442(9)	15.4582(16)
β, deg	102.117(2)	108.346(2)	92.545(4)	90	117.132(5)	113.881(10)	90
V, Å	2169.5(5)	2251.4(5)	2618.2(10)	12034(3)	6028.2(2)	4747.2(10)	4426.5(6)
Z	4	4	4	12	4	4	6
T, K	100(2)	100(2)	100(2)	200(2)	100(2)	100(2)	100(2)
ρ calcd, g cm^{-3}	1.477	1.311	1.592	1.181	1.259	1.526	1.361
refl. collected/$2\Theta_{max}$	29229/60.06	70150/64.50	73852/61.68	43776/56.62	97887/50.00	67625/56.10	46999/66.70
unique refl./I > 2σ(I)	3179/2675	7968/7038	8197/7491	3340/2748	10614/8496	11456/8218	1915/1730
no. of params/restr.	151/0	268/0	363/0	148/0	730/0	657/0	67/0
λ, Å /μ(Kα), cm^{-1}	0.71073/5.68	0.71073/5.40	0.71073/5.80	0.71073/3.22	0.71073/2.63	0.71073/4.07	0.71073/4.25
R1[a]/goodness of fit[b]	0.0355/1.089	0.0275/1.030	0.0517/1.187	0.0446/1.013	0.0659/1.087	0.0528/1.078	0.0402/1.094
*w*R2[c] ($I > 2\sigma(I)$)	0.0899	0.0759	0.1270	0.1043	0.1479	0.0978	0.1107
residual density, e$Å^{-3}$	+0.50/−0.48	+0.50/−0.43	+0.73/−0.47	+0.43/−0.28	+1.07/−0.49	+0.36/−0.60	+0.52/−0.74

[a]Observation criterion: $I > 2\sigma(I)$. $R1 = \Sigma||F_o| - |F_c||/\Sigma|F_o|$. [b]$GOF = [\Sigma[w(F_o^2 - F_c^2)^2]/(n-p)]^{1/2}$. [c]$wR2 = [\Sigma[w(F_o^2 - F_c^2)^2]/\Sigma[w(F_o^2)^2]]^{1/2}$ where $w = 1/\sigma^2(F_o^2) + (aP)^2 + bP$, $P = (F_o^2 + 2F_c^2)/3$.

dx.doi.org/10.1021/ic302743s | Inorg. Chem. 2013, 52, 4472−4487

unable to grow high quality crystals of this complex, and the crystal structure of **7** serves to verify our electronic structure assignment for the former.

EXPERIMENTAL SECTION

General Considerations. Unless otherwise stated, the following syntheses were carried out under an oxygen and moisture free atmosphere using standard Schlenk techniques or a MBraun glovebox. Solvents were dried and degassed using literature procedures. The complexes $[Cr(bpy)_2(CH_3CO_2)_2]^0$ (**1**)[6] and $[Cr(bpy)(^iPrNH_2)_2(CH_3CO_2)_2]^0$ (**2**)[5], and the ligands 1,4-bis(cyclohexyl)-1,4-diaza-1,3-butadiene (DAD^0),[11] 2-(2-trifluoromethyl)anilino-4,6-di-*tert*-butylphenol $[CF_3AP]H_2$,[12] and 2,6-bis[1-(4-methoxyphenyliminoethyl)]pyridine (PDI^0)[13] were prepared as previously described. The purity of the complexes was confirmed by elemental analyses. All other reagents were purchased from Sigma-Aldrich and used without further purification.

Synthesis of Compounds. *$[Cr(bpy)_2(CH_3CO_2)_2](PF_6)$ (**3**).* A solution of $AgPF_6$ (252 mg, 1.0 mmol) in THF (10 mL) was added dropwise to a green solution of **2** (445 mg, 1.0 mmol) in THF (10 mL) and stirred for 12 h at room temperature. Subsequently, the solvent was removed in vacuo to give a brown solid that was then dissolved in CH_3CN. After filtration through Celite and removal of the solvent from the filtrate by evaporation, a red powder corresponding to **3** was obtained in 22% yield (138 mg). Alternatively, **3** could be obtained in 89% yield from the reaction of **1** with one equivalent of $AgPF_6$. X-ray quality red crystals of **3** were grown by vapor diffusion of Et_2O into a saturated acetonitrile solution of complex. Anal. Calcd. for $C_{24}H_{22}CrN_4O_4PF_6$: C, 45.94; H, 3.53; N, 8.93. Found: C, 45.62; H, 3.71; N,8.73.

*$[Cr(DAD)_3]^0$ (**4**).* Solid $CrCl_2$ (134 mg, 1.1 mmol) was added to a THF (25 mL) solution of the ligand 1,4-bis(cyclohexyl)-1,4-diaza-1,3-butadiene (DAD^0) (242 mg, 1.1 mmol) and stirred for 15 min. Subsequently, 297 mg of KC_8 (2.2 mmol) was added and the resulting dark brown slurry was stirred for a further 12 h at room temperature. The solvent was then removed by evaporation, and the residue extracted with THF. The resulting solution was filtered through a plug of Celite, and the filtrate was concentrated and cooled to −30 °C to give **4** in 38% yield (99 mg). X-ray quality crystals were grown from dilute Et_2O solutions of complex at −30 °C. ^1H NMR (C_6D_6): δ = 4.62(br), 1.84, 1.38, 1.29, 1.10, 1.01 ppm. IR (KBr disc, cm^{-1}): 2926(s), 2851(s), 1653 (w), 1596 (w), 1469 (m), 1448 (m), 1258 (m), 1213 (s), 1179 (w), 1143 (w), 1077 (w), 1017 (w), 889 (w), 750 w). M.p.: 196 °C (dec). Anal. Calcd. for $C_{42}H_{72}N_6Cr$: C, 70.74; H, 10.18; N, 11.79. Found: C, 70.26; H, 10.05; N, 11.93. μ_{eff} (294 K) = 1.1(1) μ_B.

*$[Cr(CF_3AP)_3]^0$ (**5**).* This compound was synthesized in 92% yield via an analogous procedure to its trifluoromethyl substituent-free analog.[14] X-ray quality crystals were grown by slow evaporation of solvent from a concentrated acetone solution of complex. MS (EI+): m/z 1141 $[\mathbf{5}]^+$, molecular ion peak. Anal. Calcd. for $C_{63}H_{72}CrF_9N_3O_3$: C, 66.24; H, 6.35; N, 3.68. Found: C, 66.70; H, 6.77; N, 3.72.

*$[Cr(PDI)_2](PF_6)_2$ (**6**).* A mixture of $TlPF_6$ (0.94 g, 2.7 mmol), $CrCl_2$ (0.16 g, 1.3 mmol), and acetonitrile (20 mL) was stirred for 4 h. The resulting solution of $[Cr(CH_3CN)_6](PF_6)_2$ was filtered to remove the TlCl byproduct and combined with 2 equivalents of the ligand (PDI^0) (1.00 g, 2.7 mmol). Following a further 4 h of stirring, the solvent was reduced in volume and Et_2O was added, which caused precipitation of a solid. This material was isolated by filtration, washed with Et_2O, and dried in vacuum to give **6** as a dark brown, microcrystalline material in 91% yield (1.32 g). Single crystals were grown by vapor diffusion of Et_2O into a concentrated CH_3CN solution of the complex. Anal. Calcd. for $C_{46}H_{46}CrF_{12}N_6O_4P_2$: C, 50.74; H, 4.26; N, 7.72. Found: C, 50.71; H, 4.23; N, 7.69.

*$[Cr(^{Me}bpy)_3]^0$ (**7**).* To a stirring red-brown solution of $[Cr_2(\mu\text{-}CH_3CO_2)_4]^0$ (340 mg, 1.0 mmol) in THF (20 mL) was added solid ($^{Me}bpy^0$) (737 mg, 4.0 mmol). The reaction mixture turned black in a few minutes but was stirred overnight at room temperature. Subsequently, the solution was filtered, and the black precipitate was dried under vacuum. Vapor diffusion of Et_2O into a saturated THF solution of this black material yielded X-ray quality black crystals of **7** in 27% yield (330 mg). Anal. Calcd. for $C_{36}H_{36}CrN_6$: C, 71.50; H, 6.00; N, 13.90; Cr, 8.60. Found: C, 71.18; H, 5.83; N, 13.67; Cr, 8.82.

Physical Measurements. Electronic spectra were recorded with a Perkin-Elmer Lambda 19 double-beam spectrophotometer (200−2100 nm). Variable temperature (4−300 K) magnetization data were recorded in a 1 T magnetic field using a SQUID magnetometer (MPMS quantum design). The experimental magnetic susceptibility data were corrected for underlying diamagnetism using tabulated Pascal's constants.[15] Electrochemical experiments (cyclic voltammetry) were performed using an EG&G potentiostat/galvanostat and a glassy carbon working electrode. All potentials are referenced vs. the ferricenium/ferrocene (Fc^+/Fc) couple. Chromium K-edge spectra were recorded at beamline 7-3 at the Stanford Synchroton Radiation Lightsource (SSRL) with ring conditions of 3 GeV and 350 mA. A double crystal Si(220) monochromator was used for incident energy selection, and an upstream Rh-coated collimating mirror with 9 keV energy cutoff provided harmonic rejection in combination with 30% detuning. All samples were prepared in an argon atmosphere glovebox. Complexes were diluted with boron nitride, ground to a fine powder, and pressed into 0.5 mm Al spacers. The samples were sealed between two 38 μm Kapton tape windows and maintained at 10 K during data collection in a continuous flow liquid helium cryostat. Spectra were recorded in transmission mode and represent an average of 3−5 scans. Data calibration and averaging were performed using the EXAFSPAK software package.[16a] The pre-edge and edge regions of the spectra were fit using BlueprintXAS,[16b] and normalization was achieved by setting the edge jump equal to one. The fit parameters presented represent an average of at least 30 good fits.

X-ray Crystallographic Data Collection and Refinement of the Structures. Single crystals of complexes **1**−**7** were coated with perfluoropolyether, picked up with nylon loops, and mounted in the nitrogen cold stream of the diffractometer. Graphite monochromated Mo Kα radiation (λ = 0.71073 Å) from a Mo-target rotating-anode X-ray source was used throughout. Final cell constants were obtained from least-squares fits of several thousand strong reflections. Intensity data were corrected for absorption using intensities of redundant reflections with the program SADABS.[17a] The structures were readily solved by Patterson methods and subsequent difference Fourier techniques. The Siemens ShelXTL[17b] software package was used for solution and rendering of the structures, and ShelXL97[17c] was used for the refinement. All nonhydrogen atoms were anisotropically refined, and hydrogen atoms were placed at calculated positions and refined as riding atoms with isotropic displacement parameters. Crystallographic data for all complexes are listed in Table 1.

Calculations. All DFT calculations were performed using the ORCA software package.[18] The geometries of all complexes were optimized, in redundant internal coordinates without imposing geometry constraints, and all subsequent single point calculations were performed at the B3LYP level of theory.[19] In all calculations, the def2-TZVP basis set was applied to the metal ions, nitrogen atoms, and oxygen atoms.[20] The carbon and hydrogen atoms atoms were described using the def2-TZVP basis set minus f polarization functions. Auxiliary basis sets, used to expand the electron density in the calculations, were chosen to match the orbital basis sets.[21] The RIJCOSX approximation was used to accelerate the calculations.[22] The authenticity of each converged structure was confirmed by the absence of imaginary vibrational frequencies.

Throughout this study, our computational results are described using the broken symmetry (BS) approach.[23] The following notation is used to describe the broken symmetry solutions, where the given system is divided into two fragments. The notation BS(m,n) refers to a broken symmetry state with m unpaired α-spin electrons localized on fragment 1 and n unpaired β-spin electrons localized on fragment 2. In most cases, fragments 1 and 2 correspond to the metal and the ligands, respectively. In this notation, the standard high-spin, open-shell solution is written as BS(m + n,0). The BS(m,n) notation refers to the initial guess for the wave function. The variational process does, however, have the freedom to converge to a solution of the form BS(m

dx.doi.org/10.1021/ic302743s | Inorg. Chem. 2013, 52, 4472−4487

$-n$, 0), in which the $n\beta$-spin electrons effectively pair up with $n < m$ α-spin electrons on the partner fragment. Such a solution is then a standard $M_s \cong (m - n)/2$ spin-unrestricted Kohn–Sham solution. Canonical and corresponding orbitals,[24] as well as spin density plots, were generated with the program Chimera.[25]

Time-dependent (TD-DFT) calculations of the Cr K-pre-edge for **6** were performed upon the corresponding BS(3,1) geometry optimized structure using the functional and basis sets described above but with the uncontracted CP(PPP)[26] basis set applied to the metal. These calculations allowed only for transitions from the metal 1s orbital. DFT is unable to accurately model potentials near the nucleus, which manifests in an underestimation of the absolute transition energies. As a consequence, it was necessary to apply an empirical correction of +125.22 eV. Despite the inherent limitations of this method, it has been previously demonstrated that it is quite effective at predicting the energies and relative intensities of electronic transitions originating from transition metal 1s orbitals.[27]

RESULTS

Synthesis and Characterization of Compounds. Following the procedure outlined in reference 6, involving reaction of the dimer $[Cr^{II}_2(\mu\text{-}CH_3CO_2)_4]^0$ and four equivalents of (bpy^0) in THF under strictly anaerobic conditions (eq 1), we have been able to synthesize the black mononuclear complex $[Cr(bpy)_2(CH_3CO_2)_2]^0$ (**1**). A temperature-independent magnetic moment of 2.88 μ_B in the range of 50–300 K indicates that **1** possesses an $S = 1$ ground state (Figure S1, Supporting Information). Reaction of the dimer $[Cr^{II}_2(\mu\text{-}CH_3CO_2)_4]^0$ with (bpy^0) in $^iPrNH_2$ (eq 2), or alternatively by dissolving **1** in $^iPrNH_2$ (eq 3), affords dark green crystals of $[Cr(bpy)(^iPrNH_2)_2(CH_3CO_2)_2]^0$ (**2**).[5] A temperature-independent magnetic moment of 2.81 μ_B in the range of 20–300 K was recorded for **2** (Figure S1, Supporting Information) indicating that it also has a $S = 1$ ground state.

The electronic spectra of **1** and **2** (Figure 1), which closely resemble that of $[Cr^{III}(^tbpy^\bullet)(^tbpy^0)Cl_2]^0$ ($S = 1$),[3f] are dominated by intense intraligand $\pi \rightarrow \pi^*$ transitions characteristic of the $(bpy^\bullet)^{1-}$ π-radical monoanion. The band at ~2200 nm (4400 cm^{-1}) in **1**, which is absent in **2** but present at 2325 nm in the spectra of $[Cr^{III}(^tbpy^0)(^tbpy^\bullet)Cl_2]^0$ and $[Cr(^tbpy^0)_2(^tbpy^\bullet)]^{2+}$ ($S = 1$),[3b] corresponds to a ligand-to-ligand intervalence charge transfer (LLIVCT) transition within the $\{Cr^{III}(bpy^0)(bpy^\bullet)\}$ moiety.[3f] Cumulatively, the spectroscopic data for **1** and **2** are consistent with them possessing the electronic structures $[Cr^{III}(bpy^0)(bpy^\bullet)(CH_3CO_2)_2]^0$ and $[Cr^{III}(bpy^\bullet)(^iPrNH_2)_2(CH_3CO_2)_2]^0$, respectively.

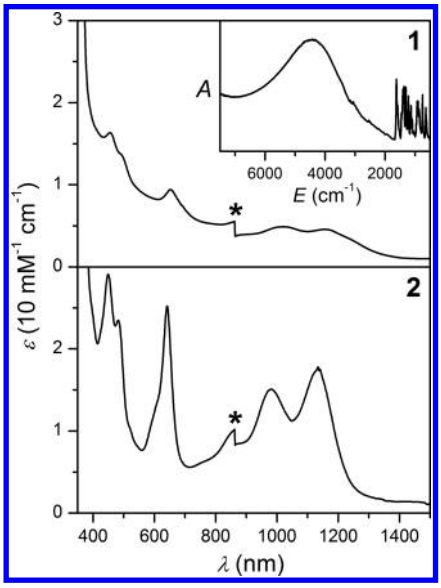

Figure 1. Electronic spectra of **1** (top) and **2** (bottom) in THF at 20 °C. The inset in the spectrum of **1** shows an IR spectrum of a KBr pellet containing solid **1** (absorption in arbitrary units). The asterisk denotes an instrument derived artifact.

Oxidation of **1** using $AgPF_6$ (eq 4) generates the complex $[Cr(bpy)_2(CH_3CO_2)_2](PF_6)$ (**3**), which has an $S = 3/2$ ground state. Its electronic spectrum, (Table 2) containing low-intensity d → d transitions at 505 nm (200 M^{-1} cm^{-1}), no $\pi \rightarrow \pi^*$ transitions associated with $(bpy^\bullet)^{1-}$, and no LLIVCT bands, is typical of an octahedral Werner-type species containing a Cr^{III} ion. The one-electron oxidation of **1** is therefore ligand centered (eq 4), and the electronic structure of **3** is $[Cr^{III}(bpy^0)_2(CH_3CO_2)_2](PF_6)$.

Table 2. Electronic Spectra of Complexes 1–7 in THF (20°C)

complex	λ, nm (ε, M^{-1} cm^{-1})
1	380 (3.1×10^4), 475 (1.4×10^4), 500 sh, 660 (0.8×10^4), 1050 (0.4×10^4), 1180 (0.4×10^4), 2200 (broad)[a]
2	380 (3.6×10^4), 480 (2.7×10^4), 500 (2.1×10^4), 640 (2.3×10^4), 990 (1.2×10^4), 1150 (1.4×10^4)
3[b]	420 sh, 505 (200)
4	393 (0.71×10^4), 439 (1.08×10^4), 514 (0.41×10^4), 534 (0.33×10^4), 630 (0.12×10^4), 773 (0.10×10^4)
5	350 sh, 446 (0.85×10^4), 523 (1.2×10^4), 660 (0.2×10^4), 720 (0.23×10^4), 800 (0.25×10^4), ~910 sh
$[\mathbf{6}]^{2+}$[b]	330 sh, 380 (6.4×10^3) sh, 500 sh, 760 (1.1×10^3), 880 (0.75×10^3), 2500 (broad)[a]
$[\mathbf{6}]^{1+}$[b]	380 sh 530 (2.4×10^3), 700 (0.8×10^3), 760 sh, 855 (1.4×10^3)
7	390 (9.3×10^3), 450 sh, 550 (2.8×10^3), 620 sh 750 sh 810 (1.8×10^3), 950 (1.7×10^3)

[a]Solid **1** in a KBr-disk (NIR spectrum). [b]CH_3CN solution.

$$[Cr^{III}(bpy^\bullet)(bpy^0)(ac)_2] \xrightarrow[AgPF_6]{THF} [Cr^{III}(bpy^0)_2(ac)_2]^+ \quad (4)$$

Reaction of $CrCl_2$ with 1 equivalent of 1,4-bis(cyclohexyl)-1,4-diaza-1,3-butadiene (DAD^0) in THF followed by addition of KC_8 as reductant afforded dark brown microcrystals of neutral $[Cr(DAD)_3]^0$ (**4**) in 38% yield. Its electronic spectrum (Table 2) closely resembles that of neutral $[Cr^{III}(\alpha\text{-diimine}^\bullet)(acac)_2]^0$,[29] where $(\alpha\text{-diimine}^\bullet)^{1-}$ represents the one-electron reduced π-radical anion derived from 2,3-dimethyl-1,4-bis(2,6-diisopropyl-phenyl)-1,4-diaza-1,3-butadiene. We take this as a first indication that complex **4** contains three $(DAD^\bullet)^{1-}$ π-radical anions and a Cr^{III} ion. A magnetic susceptibility measurement at ambient temperature revealed a magnetic moment (1.1 μ_B) suggestive of very weak paramagnetism, as previously observed for $[Cr^{III}(^tbpy^\bullet)_3]^0$.[3b] In C_6D_6 solution **4** exhibits a "normal" ^1H NMR spectrum (see Experimental Section) indicative of an $S = 0$ ground state.

A similar complex has been described by us previously, $[Cr^{III}(AP^\bullet)]^0$ ($S = 0$),[14] in which three monoanionic π-radical ligands obtained from one-electron oxidation of deprotonated 2-anilino-4,6-di-*tert*-butylphenol $H_2(AP)$ are *N,O*-coordinated to a Cr^{III} ion. In this study, we used the closely related ligand $H_2(CF_3AP)$, 2-(2-trifluoromethyl)-anilino-4,6-di-*tert*-butylphenol, to prepare the red-black complex $[Cr(CF_3AP)_3]^0$ (**5**) by heating a mixture of $Cr^{III}(THF)_3Cl_3$, NEt_3, and $H_2(CF_3AP)$ in CH_3CN solution under air. The temperature dependence of

dx.doi.org/10.1021/ic302743s | Inorg. Chem. 2013, 52, 4472–4487

the effective magnetic moment of **5** in the range of 30−300 K displays a monotonic increase of μ_{eff} with increasing temperature from 0.4 μ_B at 10 K to 1.0 μ_B at 300 K. It is possible to fit this temperature dependence with the Heisenberg−Dirac-van Vleck spin Hamiltonian operator (eq 5) by using a single antiferromagnetic coupling constant J of approximately −500 cm^{-1} to model an interaction between an $S = 3/2$ Cr^{III} ion and three $S = 1/2$ iminosemiquinonate ligands ($S_{Cr} = 3/2$; $S_i = 1/2$; $i = 1, 2, 3$).

$$\hat{H} = -2J \sum_i S_{Cr} \cdot S_i \qquad (5)$$

Reaction of $[Cr^{II}_2(\mu\text{-}CH_3CO_2)_4]$ in THF with 4 equivalents of (^{Me}bpy^0) under anaerobic conditions unexpectedly produced black crystals of the neutral complex $[Cr(^{Me}bpy)_3]^0$ (**7**) in low yield. The stoichiometry of this reaction is currently unknown. However, black single crystals of **7** suitable for X-ray crystallography were obtained by vapor diffusion of diethyl ether into a saturated THF solution of the complex; and it was found to be effectively diamagnetic (μ_{eff} = 0.49 μ_B) over the temperature range of 5−300 K (Figure S1, Supporting Information).

The reaction of $[Cr^{II}(CH_3CN)_6](PF_6)_2$ in acetonitrile with 2 equivalents of the ligand 2,6-bis[1-(4-methoxyphenylimino)-ethyl]pyridine (PDI^0) (see Chart 1), under strictly anaerobic conditions, followed by addition of diethyl ether produced a dark brown microcrystalline precipitate of $[Cr(PDI)_2](PF_6)_2$ (**6**) in 91% yield. This complex displays a temperature-independent (10−300 K) magnetic moment of 2.83 μ_B (Figure S2, Supporting Information), thereby indicating that it possesses a triplet ($S = 1$) ground state. Figure 2 displays the

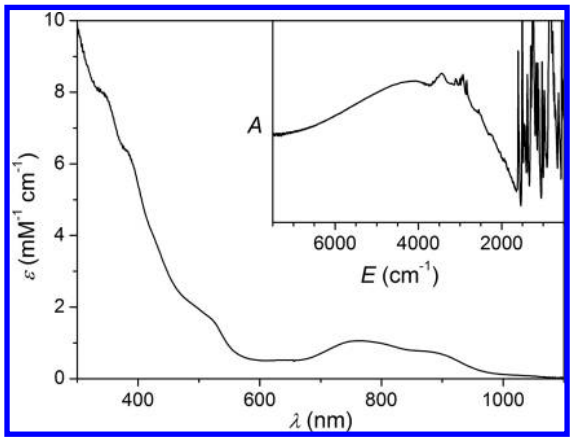

Figure 2. Electronic spectrum of **6** in CH_3CN solution at 20 °C. The inset shows the IR spectrum of a solid sample of **6** measured as a KBr pellet (absorption in arbitrary units).

electronic spectrum of **6** in the range of 300−1100 nm (33300−9090 cm^{-1}) dissolved in acetonitrile and, as an inset, the solid as a KBr pellet in the range of 7000−1000 cm^{-1} (1430−10000 nm). The intense features at 500, 750, and 880 nm ($\varepsilon > 10^3$ L mol^{-1} cm^{-1}) can be assigned to intraligand $\pi \rightarrow \pi^*$ transitions associated with a $(PDI^{\bullet})^{1-}$ radical, whereas the very broad band centered at ∼2500 nm (4000 cm^{-1}) derives from a LLIVCT transition. The breadth of the latter is suggestive of class I or II (localized) behavior, a phenomenon that has been observed in a number of other ligand mixed valence compounds, such as $[Cr^{III}(bpy^{\bullet})(bpy^0)X_2]^0$ ($S = 1$) (X = Cl, NCS, acetate).[3f]

X-ray Crystallography. With the exception of **4**, which was measured at 200(2) K, the high resolution crystal structures of **1**−**7** were recorded at 100(2) K. Selected bond distances are summarized in Table 3, and the corresponding structures are displayed in Figures 3−8. The picture that emerges is fully consistent with the data presented in the previous section and solidifies the electronic structure assignments proposed therein.

The structure of the neutral complex **2** (Figure 3) consists of a 6-coordinate Cr center ligated by a single *N,N′*-coordinated bpy, two neutral monodentate ^{i}PrNH$_2$ ligands coordinated *trans* to one another, and two *cis*-oriented monodentate acetates. The bpy $C_{py}-C_{py}$ and C−N chelate bond distances are very similar to those of the uncoordinated radical anion in $K(bpy^{\bullet})(en)$[7] and clearly show that the oxidation level of the bpy ligand is that of a π-radical anion. This reinforces the $[Cr^{III}(bpy^{\bullet})(^iPrNH_2)_2(CH_3CO_2)_2]^0$ electronic structure assignment suggested in the previous section.

Complex **3** consists of the monocation $[Cr^{III}(bpy^0)_2(CH_3CO_2)_2]^{1+}$ (Figure 4) and a PF_6^- counter monoanion. The acetate ligands are oriented *cis* relative to one another, and the bpy ligands display C−C and C−N bond lengths (Table 3) typical of (bpy^0). Note that both (bpy^0) ligands are crystallographically independent in this structure, but the reverse is true in *cis*-$[Cr^{III}(bpy^0)_2Cl_2](Cl)_{0.38}(PF_6)_{0.62}$.[28] In contrast to **3**, the Cr center in **1** lies on a crystallographic 2-fold symmetry axis (C_2), thereby rendering both bpy ligands identical. Notably, the C−C and C−N bond distances in **1** are intermediate between those in **3** and **2** (see Table 4), which contain two neutral (bpy^0) ligands and a single $(bpy^{\bullet})^{1-}$ π-radical anion, respectively. Two different models may be employed to explain this: (a) **1** possesses the localized electronic structure $[Cr^{III}(bpy^0)(bpy^{\bullet})(CH_3CO_2)_2]^0$, but static disorder prevails in the solid-state and renders the two bpy ligands equivalent; or (b) a truly delocalized model represented by the two resonance structures $[Cr^{III}(bpy^0)(bpy^{\bullet})(CH_3CO_2)_2]^0 \leftrightarrow [Cr^{III}(bpy^{\bullet})(bpy^0)(CH_3CO_2)_2]^0$ is most appropriate. However, the crystallographically observed C−C and C−N bond lengths exclude a third possibility describing **1** as $[Cr^{II}(bpy^0)_2(CH_3CO_2)_2]^0$.

Complex **4** is a neutral species, possessing crystallographic D_3 symmetry, which is composed of a Cr ion coordinated to three equivalent DAD ligands (Figure 5). The respective C−C and average C−N bond lengths in the $Cr(N_2C_2)$ chelates of 1.389(2) and 1.331(2) Å closely resemble those in $[Cr^{III}(\alpha\text{-diimine}^{\bullet})(acac)_2]^0$ [29a] and are typical for the one-electron reduced form of α-diimines.[29] Thus, the electronic structure of **4** is best described as $[Cr^{III}(DAD^{\bullet})_3]^0$, wherein the spin of the three unpaired electrons of the $(DAD^{\bullet})^{1-}$ radicals are intramolecularly antiferromagnetically coupled to the three unpaired electrons of the Cr^{III} ion to give the experimentally observed singlet ground state.

Complex **5** is also a neutral species (Figure 6) containing a Cr ion and three bidentate ligands, in this case aminophenolates. The structural parameters of the three equivalent, but crystallographically independent, ligands in **5** are essentially the same as those in the previously published structure of $[Cr^{III}(AP^{\bullet})_3]^0$ (where $(AP^{\bullet})^{1-}$ is the radical anion of 2-anilino-4,6-di-*tert*-butylphenolate).[14] Additionally, the C−O and C−N distances are very similar to those reported for the free radical 4,6-di-*tert*-butyl-2-*tert*-butyliminosemiquinone.[30] Hence, the electronic structure of this complex is best described as $[Cr^{III}(CF_3AP^{\bullet})_3]^0$, with the observed $S = 0$ ground state once

dx.doi.org/10.1021/ic302743s | Inorg. Chem. 2013, 52, 4472−4487

Table 3. Selected Bond Lengths (Å) from the Crystal Structures of 1−7

Complex 1							
Cr−O(21)	1.969(1)	C(4)−C(5)	1.381(2)	Cr−N(12)	2.030(1)	C(5)−C(6)	1.394(2)
Cr−N(1)	2.043(1)	C(6)−C(7)	1.454(2)	N(1)−C(2)	1.357(2)	C(7)−N(12)	1.362(2)
N(1)−C(6)	1.369(2)	C(7)−C(8)	1.401(2)	C(2)−C(3)	1.375(2)	C(8)−C(9)	1.377(2)
C(3)−C(4)	1.394(2)	C(9)−C(10)	1.401(2)	C(11)−N(12)	1.355(2)	C(10)−C(11)	1.377(2)
O(21)−C(22)	1.291(2)	C(22)−O(23)	1.232(2)	C(22)−C(24)	1.510(2)		
Complex 2							
Cr−O(21)	1.9778(7)	N(1)−C(2)	1.364(1)	N(12)−C(11)	1.364(1)	Cr−O(31)	1.9842(7)
N(1)−C(6)	1.384(1)	N(12)−C(7)	1.384(1)	Cr−N(1)	1.9983(8)	C(5)−C(6)	1.414(1)
C(11)−C(10)	1.370(1)	Cr−N(12)	1.9987(8)	C(5)−C(4)	1.374(1)	C(10)−C(9)	1.415(2)
Cr−N(51)	2.0943(8)	C(4)−C(3)	1.415(1)	C(9)−C(8)	1.370(1)	Cr−N(41)	2.1083(8)
C(3)−C(2)	1.367(1)	C(8)−C(7)	1.412(1)	C(7)−C(6)	1.421(1)		
Complex 3							
Cr−O(51)	1.922(2)	N(1)−C(2)	1.339(3)	C(10)−C(11)	1.387(3)	Cr−O(41)	1.932(2)
N(1)−C(6)	1.356(3)	C(11)−N(12)	1.342(3)	Cr−N(12)	2.054(2)	C(2)−C(3)	1.386(3)
N(21)−C(22)	1.341(2)	Cr−N(21)	2.056(2)	C(3)−C(4)	1.385(3)	N(21)−C(26)	1.355(2)
C(4)−C(5)	1.376(3)	Cr−N(32)	2.073(2)	C(5)−C(6)	1.395(3)	C(22)−C(23)	1.388(3)
Cr−N(1)	2.076(2)	C(6)−C(7)	1.470(3)	C(23)−C(24)	1.380(3)	C(28)−C(29)	1.385(3)
C(7)−N(12)	1.352(3)	C(24)−C(25)	1.389(3)	C(29)−C(30)	1.388(3)	C(7)−C(8)	1.392(3)
C(25)−C(26)	1.383(3)	C(30)−C(31)	1.385(3)	C(8)−C(9)	1.374(4)	C(26)−C(27)	1.474(3)
C(31)−N(32)	1.347(2)	C(27)−C(28)	1.390(3)	C(27)−N(32)	1.355(2)	C(9)−C(10)	1.382(4)
Complex 4							
Cr−N(1)	2.036(1)	N(2)−C(2)	1.330(2)	Cr−N(2)	2.040(1)	N(2)−C(14)	1.476(2)
N(1)−C(1)	1.332(2)	C(1)−C(2)	1.389(2)	N(1)−C(8)	1.475(2)		
Complex 5							
Cr−O(1)	1.922(2)	Cr−O(31)	1.942(2)	Cr−O(61)	1.965(2)	Cr−N(7)	2.004(3)
Cr−N(37)	2.024(3)	Cr−N(67)	2.034(3)	O(1)−C(1)	1.305(4)	C(1)−C(2)	1.432(4)
C(1)−C(6)	1.433(5)	C(2)−C(3)	1.374(5)	C(2)−C14	1.533(5)	C(3)−C(4)	1.422(5)
C(4)−C(5)	1.368(5)	C(5)−C(6)	1.413(5)	C(6)−N(7)	1.362(4)	N(7)−C(8)	1.422(4)
O(31)−C(31)	1.295(4)	C(31)−C(32)	1.433(4)	C(31)−C(36)	1.436(4)	C(32)−C(33)	1.364(5)
C(32)−C(44)	1.532(4)	C(33)−C(34)	1.428(5)	C(34)−C(35)	1.372(4)	C(35)−C(36)	1.413(4)
C(36)−N(37)	1.359(4)	N(37)−C(38)	1.437(4)	O(61)−C(61)	1.304(4)	C(61)−C(62)	1.418(4)
C(61)−C(66)	1.438(4)	C(62)−C(63)	1.378(5)	C(63)−C(74)	1.535(4)	C(63)−C(64)	1.429(5)
C(64)−C(65)	1.360(5)	C(65)−C(66)	1.414(4)	C(66)−N(67)	1.350(4)	N(67)−C(68)	1.424(4)
Complex 6							
Cr−N(38)	1.917(2)	Cr−N(8)	1.985(2)	Cr−N(40)	2.028(2)	Cr−N(10)	2.066(2)
Cr−N(31)	2.074(2)	Cr−N(1)	2.091(2)	N(1)−C(2)	1.302(3)	N(1)−C(21)	1.437(3)
C(2)−C(20)	1.488(4)	C(2)−C(3)	1.493(4)	C(3)− N(8)	1.341(3)	C(3)−C(4)	1.386(4)
C(4)−C(5)	1.394(4)	C(5)−C(6)	1.383(4)	C(6)−C(7)	1.390(3)	C(7)−N(8)	1.346(3)
C(7)−C(9)	1.474(4)	C(9)−N(10)	1.309(3)	C(9)−C(19)	1.488(3)	N(10)−C(11)	1.446(3)
N(31)−C(32)	1.321(3)	N(31)−C(51)	1.431(3)	C(32)−C(33)	1.451(4)	C(32)−C(50)	1.493(4)
C(33)−N(38)	1.367(3)	C(33)−C(34)	1.389(3)	C(34)−C(35)	1.397(4)	C(35)−C(36)	1.380(4)
C(36)−C(37)	1.400(4)	C(37)−N(38)	1.369(3)	C(37)−C(39)	1.440(4)	C(39)−N(40)	1.322(3)
C(39)−C(49)	1.494(4)	N(40)−C(41)	1.443(3)				
Complex 7							
Cr−N(1)	2.018(1)	N(1)−C(6)	1.384(1)	C(3)−C(4)	1.415(2)	C(4)−C(7)	1.501(2)
N(1)−C(2)	1.361(1)	C(2)−C(3)	1.372(2)	C(4)−C(5)	1.378(2)	C(6)−C(6A)	1.426(2)

again being obtained by antiferromagnetic coupling of the unpaired spins of the ligand radicals with the Cr^{III} center.

Figure 7 displays the structure of $[Cr(PDI)_2]^{2+}$, the dication component of complex **6**. The summary of its bond lengths in Table 3 clearly shows that the two tridentate pyridine-2,6-diimine ligands are *not* equivalent, with one displaying structural features similar to those previously observed in $[Mn^{II}(PDI^0)_2]^{2+}$ and the other to $[Mn^{III}(PDI^{\bullet})_2]^{1+}$.[31] In other words, the $C_{imine}-N_{imine}$, $C_{imine}-C_{py}$, and $C_{py}-N_{py}$ bond lengths of one ligand are typical of (PDI^0) and those of the other of $(PDI^{\bullet})^{1-}$ (see Scheme 1). This renders the oxidation state of the central Cr ion in **6** +III and is consistent with the electronic description $[Cr^{III}(PDI^0)(PDI^{\bullet})]^{2+}$. The observation of distinct oxidation states for the two PDI ligands allows this complex to be classified as Class 1 in the solid state (i.e., it has a localized electronic structure).

Finally, we have been able to obtain a crystal structure of neutral $[Cr(^{Me}bpy)_3]$ (**7**, Figure 8). This complex contains three crystallographically symmetry-related *N*,*N*′-coordinated ligands that have C−C and C−N distances very similar to those observed in the crystal structures of **2** and K(bpy•)(en) (en = ethylenediamine),[7] which are indicative of $(^{Me}bpy^{\bullet})^{1-}$ radical anions. This leads to formulation of the electronic structure of **7** as $[Cr^{III}(^{Me}bpy^{\bullet})_3]$. The twist angle of 49.3° indicates that the

dx.doi.org/10.1021/ic302743s | Inorg. Chem. 2013, 52, 4472−4487

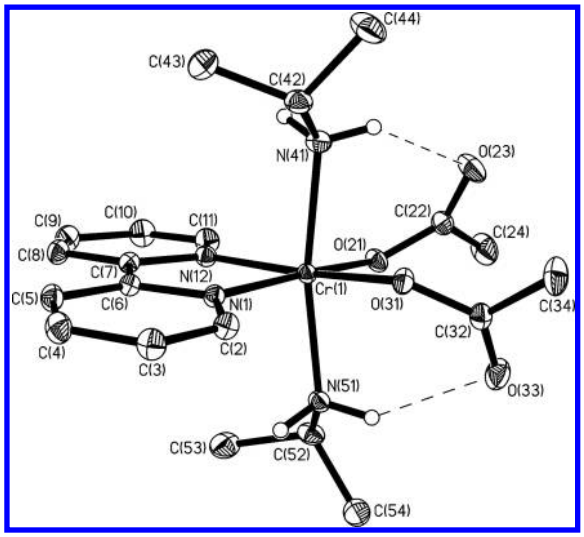

Figure 3. Molecular structure of complex **2** depicted using 50% probability ellipsoids. Hydrogen atoms omitted for clarity.

CrN_6 polyhedron is a nearly regular octahedron. Gratifyingly, the calculated optimized geometry of $[Cr^{III}(^tbpy^{\bullet})_3]^0$, which has been structurally characterized only by EXAFS,[3b] is superimposable with the experimentally determined structure of **7**. For example, the crystallographically determined average Cr−N distance at 2.0183(10) Å in **7** is, within experimental error, identical to the value of 2.00 ± 0.24 Å determined by EXAFS for $[Cr^{III}(^tbpy^{\bullet})_3]^0$. From the calculated electronic structure of $[Cr^{III}(^tbpy^{\bullet})_3]^0$, it was established that the observed singlet ground state of this complex, and by extension that of **7**, derives from strong antiferromagnetic coupling of three paramagnetic $(^tbpy^{\bullet})^{1-}$ ligands with the d^3 Cr^{III} center.

Electro- and Spectrochemical Investigations. Cyclic voltammograms (CV) of complexes **5** and **6** have been recorded in CH_3CN solution using 0.10 M $[N(n\text{-}Bu)_4]PF_6$ as supporting electrolyte, a glassy carbon working electrode, and a $Ag/AgNO_3$ reference electrode. The resulting traces can be found in Figure S3 (Supporting Information) and Figure 9, respectively, and the potentials ($E_{1/2}$) of the redox couples therein are listed in Table 4. All quoted potentials are referenced versus the ferricenium/ferrocene couple (Fc^+/Fc).

The CV of **5** displays five reversible one-electron redox couples and is nearly identical to that previously reported for $[Cr^{III}(AP^{\bullet})_3]^0$.[14] Indeed, the $E_{1/2}$ $^{1-5}$ redox potentials of both complexes are comparable, which indicates that the introduction of CF_3 substituents had a minimal impact upon the electronic properties of the complex. On this basis and the previous assignment of the CV of $[Cr^{III}(AP^{\bullet})_3]^0$, all one-electron redox processes observed for **5** can be assumed to be ligand based (eq 6, where $(IBQ)^0$ = iminobenzoquinone; $(AP^{\bullet})^{1-}$ = iminobenzosemiquinone; $(AP)^{2-}$ = iminocatecholate).

The CV of **6** in acetonitrile (Figure 9) displays four fully reversible one-electron transfer waves (one oxidation and three reductions), which we assign to the redox couples outlined in eq 7. Thus, all redox processes are again ligand centered and involve successive reduction of the neutral (PDI^0) ligand to π-radical anions and subsequently dianions (Scheme 1). The

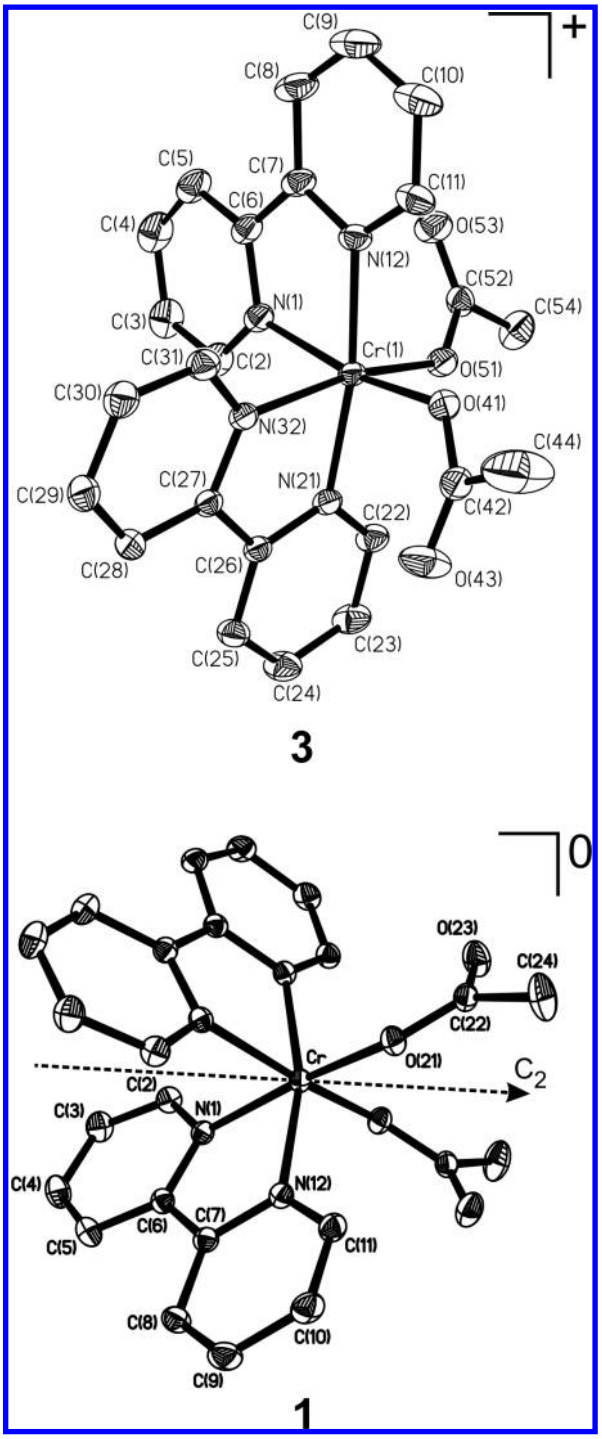

Figure 4. Structure of the monocation in crystals of **3** depicted using 50% probability ellipsoids (top) and neutral **1** (bottom). Hydrogen atoms and the counteranion in the former have been omitted for clarity.

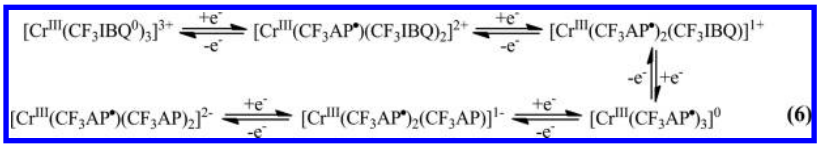

dx.doi.org/10.1021/ic302743s | Inorg. Chem. 2013, 52, 4472−4487

Table 4. Redox Potentials ($E_{1/2}$) of Complexes in Acetonitrile Solution (25°C)[a]

complex	3+/2+	2+/1+	1+/0	0/1−	1−/2−
5	1.27	0.80	0.08	−1.18	−1.74
$[Cr(AP^{\bullet})_3]^{0}$ [b]	1.10	0.64	−0.10	−1.26	−1.77
6	−0.09	−0.60	−1.40	−2.46	

[a] $E_{1/2}$ in volts vs Fc^+/Fc (CH_3CN solution containing 0.10 M $[N(n\text{-}Bu)_4]PF_6$); scan rate, 200 mV s^{-1}. [b] Reference 14.

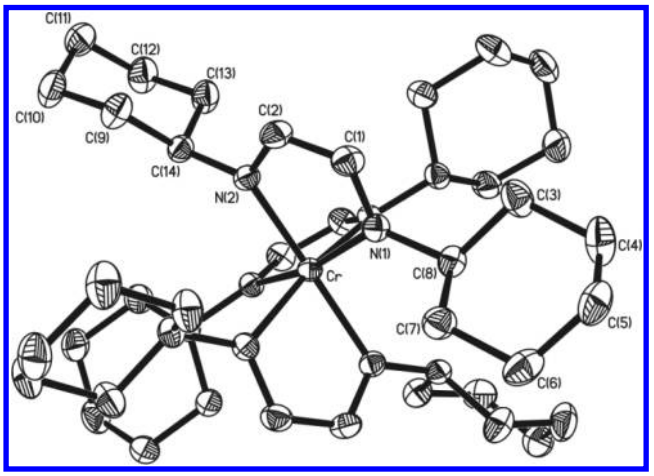

Figure 5. Molecular structure of complex **4** depicted using 50% probability ellipsoids. Hydrogen atoms have been omitted for clarity.

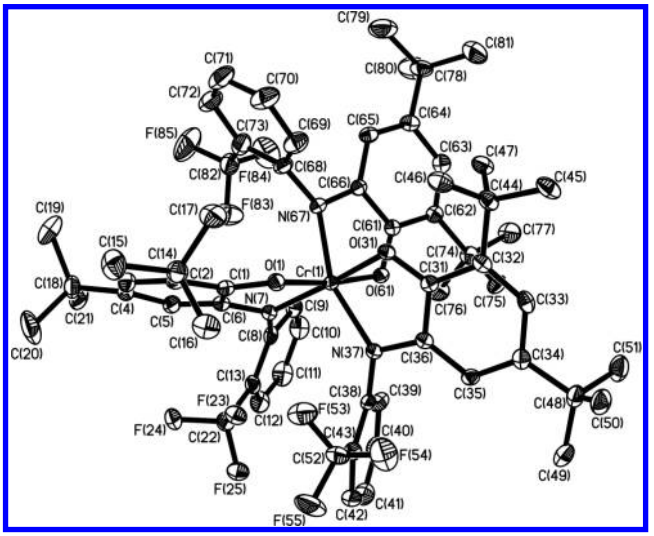

Figure 6. Molecular structure of complex **5** depicted using 40% probability ellipsoids. Hydrogen atoms have been omitted for clarity.

latter can coordinate as either a ground state triplet $(PDI^{\bullet\bullet})^{2-}$ and or an excited state singlet $(PDI^{2-})^{2-}$.[32]

Figure 10 displays the electronic spectra of the dicationic, monocationic, and neutral variants of **6**, which were generated by coulometry. The spectra clearly show the presence of coordinated $(PDI^{\bullet})^{1-}$ ligands, namely, three intense (ε > 1000

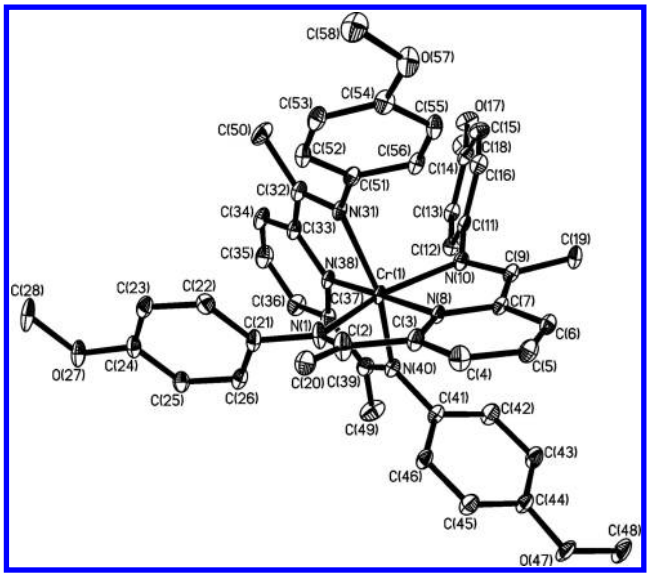

Figure 7. Structure of the dication in crystals of **6** depicted using 40% probability ellipsoids. Hydrogen atoms and counteranions have been omitted for clarity.

Scheme 1. Experimental C−C and C−N Bond Distances in (PDI^0), $(PDI^{\bullet})^{1-}$, and Those Calculated for $(PDI^{\bullet\bullet})^{2-}$ in Å[a]

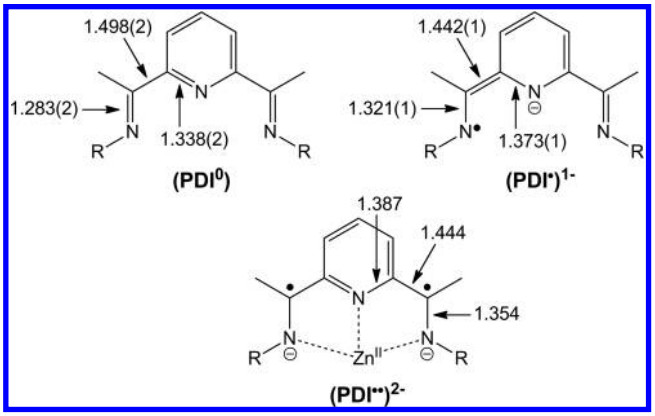

[a] Only one resonance structure is depicted in each case. Reprinted from refs 31 and 32. Copyright 2000 and 2006, respectively, American Chemical Society.

M^{-1} cm^{-1}) transitions at ~520 nm, ~800 nm, and 920 nm, that increase in intensity with decreasing charge, which is suggestive of sequential ligand-centered reductions On this basis, we propose the following ground states: S = 3/2 for the trication, S = 1 for the dication (measured by SQUID), S = 1/2 for the monocation, and S = 0 for the neutral species. The electronic structure proposed for the latter is analogous to that of $[Cr^{III}(terpy^{\bullet})(terpy^{\bullet\bullet})]^0$ (S = 0), where $(terpy^{\bullet})^{1-}$ corresponds to the singly reduced (S = 1/2) form of the tridentate ligand 2,2′:6,2″-terpyridine, and $(terpy^{\bullet\bullet})^{2-}$ is the dianion in its triplet (S = 1) excited state.[3d]

$$[Cr^{III}(PDI^0)_2]^{3+} \underset{-e^-}{\overset{+e^-}{\rightleftharpoons}} [Cr^{III}(PDI^0)(PDI^{\bullet})]^{2+} \underset{-e^-}{\overset{+e^-}{\rightleftharpoons}} [Cr^{III}(PDI^{\bullet})_2]^{1+}$$
$$-e^- \Big\downarrow \Big\uparrow +e^-$$
$$[Cr^{III}(PDI^{\bullet\bullet})(PDI^{\bullet\bullet})]^{1-} \underset{+e^-}{\overset{-e^-}{\rightleftharpoons}} [Cr^{III}(PDI^{\bullet})(PDI^{\bullet\bullet})]^0 \quad (7)$$

dx.doi.org/10.1021/ic302743s | Inorg. Chem. 2013, 52, 4472−4487

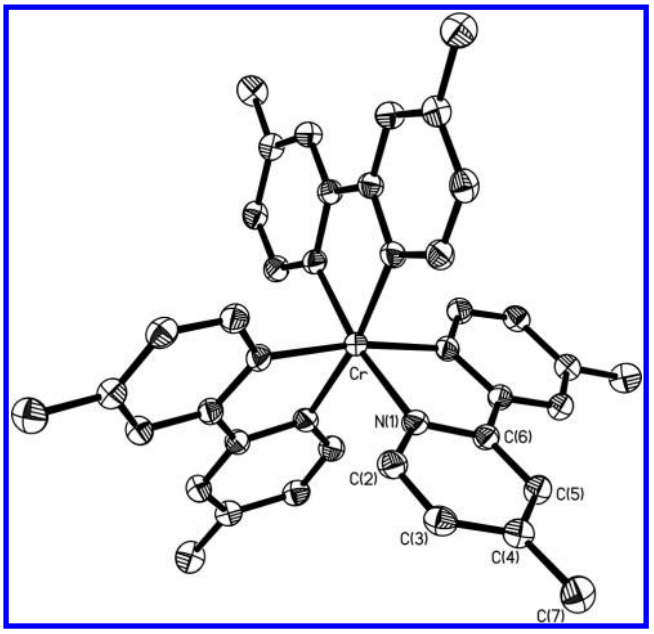

Figure 8. Molecular structure of **7** depicted using 50% probability ellipsoids. Hydrogen atoms have been omitted for clarity.

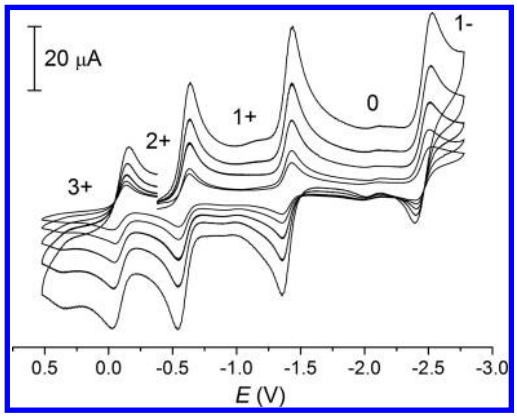

Figure 9. Cyclic voltammogram of a CH_3CN solution of **6** containing 0.20 M $[N(n\text{-}Bu)_4]PF_6$ electrolyte at 20 °C. Potentials are referenced vs. the ferrocenium/ferrocene (Fc^+/Fc) couple. Scan rates: 50, 100, 200, 400, and 800 mV s^{-1}.

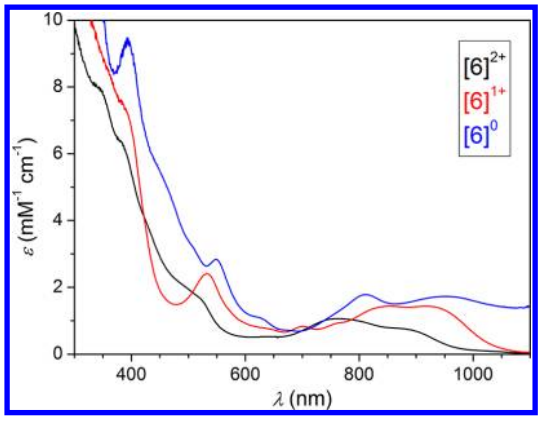

Figure 10. Electronic spectra of the electrochemically generated dication (black), monocation (red), and neutral (blue) variants of complex **6** in CH_3CN solution containing 0.20 M $[N(n\text{-}Bu)_4]PF_6$ as electrolyte.

Chromium K-Edge X-ray Absorption Spectroscopy of Compounds. As pointed out in a number of recent publications,[3b,d,f,8b] XAS is a very useful tool for comparing metal oxidation state across a series of chromium complexes. For example, Cr K-edge XAS has provided definitive evidence that all members of the electron transfer series $[Cr(bpy)_3]^{3+/2+/1+/0}$ and $[Cr(terpy)_2]^{3+/2+/1+/0}$ contain a high-spin Cr^{III} ion and by extension that all redox processes are ligand-centered.[3b,d] It has been found that in octahedral Cr^{III} complexes, regardless of the nature of the six donor atoms, the lowest energy pre-edge transition (1s → 3d) occurs in the narrow range of 5989.9−5990.7 eV. In contrast, in genuine low- or high-spin Cr^{II} species this transition is found at 5988.7−5989.2 eV.[3b,d,f]

In this study, we have measured the XAS spectra of compounds **2**, **4**, **5**, and **6**, the results of which are presented in Table 5 and Figure 11. For reference, the Cr K-edge data for

Table 5. Experimentally Determined Cr K-(pre)edge Energies (eV) of Selected Cr Complexes

complex	energy (eV)	reference
2	5990.4, 5992.5, 5994.7	this work
4	5990.5, 5992.4, 5994.2(1)	this work
5	5990.5, 5992.4, 5994.2(1)	this work
6	5989.7, 5990.6(1), 5992.4, 5994.3(1)	this work
trans-$[Cr^{III}Cl_2(OH_2)_4]Cl$	5990.6, 5992.7	3b, 7
$[Cr^{III}(tacn)_2]^{3+}$	5990.4, 5992.7	3b
$[Cr^{II}(tacn)_2]^{2+}$	5988.4, 5989.3	3b
$[Cr^{II}(CN)_6]K_2$	5989.1, 5991.0	3b
$[Cr^{III}(CN)_6]K_3$	5990.2, 5990.9	3b
$[Cr^{III}(terpy^0)_2]^{3+}$	5990.3, 5992.9	3d
$[Cr^{III}(terpy^\bullet)(terpy^0)]^{2+}$	5989.9, 5991.0	3d
$[Cr^{III}Cl_2(bpy^0)_2]^+$	5990.4	3f
$[Cr^{III}Cl_2(^tbpy^\bullet)(^tbpy^0)]^0$	5990.4	3f
$[Cr^{III}(^tbpy^\bullet)_3]^0$	5990.4	3b

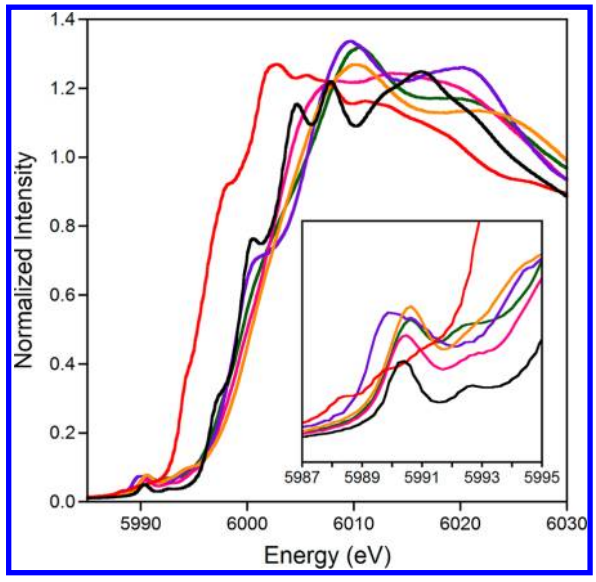

Figure 11. Cr K-edge X-ray absorption spectra of the following complexes: $[Cr^{III}(tacn)_2]^{3+}$ (black); $[Cr^{II}(tacn)_2]^{2+}$ (red); $[Cr^{III}(bpy^\bullet)(CH_3CO_2)_2(^iPrNH_2)_2]^0$ **2** (pink); $[Cr^{III}(DAD^\bullet)_3]^0$ **4** (green); $[Cr^{III}(PDI^0)(PDI^\bullet)]^{2+}$ **6** (blue); and $[Cr^{III}(CF_3AP^\bullet)_3]^0$ **5** (orange). The inset contains an expansion of the pre-edge region.

dx.doi.org/10.1021/ic302743s | Inorg. Chem. 2013, 52, 4472−4487

$[Cr^{II}(tacn)_2]^{2+}$ and $[Cr^{III}(tacn)_2]^{3+}$ (where tacn = 1,4,7-triazacyclononane) are included. On the basis of the comparison to the rising edge inflection points of the tacn complexes, it is clear that compounds **2**, **4**, **5**, and **6** all fall into the Cr^{III} energy range. Further evidence for this oxidation state assignment can also be derived from the 1s → 3d pre-edge transitions. The first pre-edge peaks of **2**, **4**, and **5** are all positioned in the narrow range of 5990.4−5990.5 eV at energies comparable to those of $[Cr^{III}(tacn)_2]^{3+}$ (5990.3 eV),[3b] $[Cr^{III}(^tbpy)_3]^{3+}$ (5990.4 eV),[3b] and $[Cr^{III}(mnt)_3]^{3-}$ (5990.3 eV)[33] (where $(mnt)^{2-}$ = maleonitrile dithiolate) and consistent with the presence of a central Cr^{III} ion.

In contrast, the pre-edge region of complex **6** displays two peaks at 5989.7 and 5990.6(1) eV (Figure 12). The former

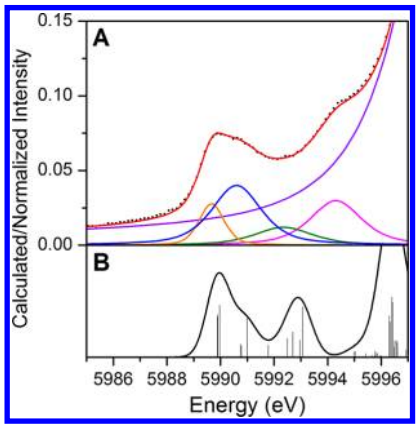

Figure 12. Cr K-pre-edge X-ray absorption spectrum of **6**: (A) Experimental spectrum (black dots) with deconvoluted maxima in orange, blue, green and magenta, and the sum of the four maxima in red. (B) The corresponding TD-DFT simulated spectrum. The bars represent calculated transitions and their relative intensities (see Supporting Information for further information).

value falls outside of the region usually associated with Cr^{III} but is at too high of an energy for classification as Cr^{II}. In response to these observations, time-dependent DFT calculation of the pre-edge XAS spectrum of **6** was undertaken using atomic coordinates taken from a BS(3,1) geometry optimized structure of this complex, which contains a Cr^{III} center coordinated to a ligand radical (see below for further details). This simulation also displayed two distinct low-energy pre-edge features that were found to correspond to 1s → 3d transitions (see Figure S15, Supporting Information). In other Cr^{III} XAS spectra, these two features overlap.

DFT Calculations. We have calculated the electronic structures of complexes **1**−**6** and, for calibration purposes, $[Co^{III}(AP^{\bullet})_3]^0$ (S = 3/2)[34] by using (broken symmetry) DFT. These calculations were performed using atomic coordinates of both geometry optimized and X-ray structures. Other than a slight overestimation of the chromium-to-ligand bond lengths (by up to 0.07 Å), which is typically observed with the B3LYP functional, the agreement between the calculated and experimental structures was found to be excellent. Furthermore, the electronic structure descriptions obtained with both starting geometries were qualitatively identical.

The electronic structure of the complex $[Co^{III}(AP^{\bullet})_3]^0$ has been demonstrated by X-ray crystallography to contain a low-spin Co^{III} ion (d^6, S = 0) and three paramagnetic $(AP^{\bullet})^{1-}$ iminosemiquinone ligands (S = 1/2), which are produced by one-electron oxidation of *N*-phenyl-3,5-di-*tert*-butyl-aminophenol.[34] Magnetochemical studies revealed that this compound possesses a S = 3/2 ground state, which is separated by only 27 cm^{-1} from an energetically close-lying S = 1/2 excited state, stemming from intramolecular ferromagnetic coupling of the three π-radical anion ligands ($J_{12} = J_{23}$ = +9.1 cm^{-1} and J_{13} = +59.5 cm^{-1}, giving J_{av} = +26 cm^{-1}).

The qualitative frontier molecular orbital (FMO) picture obtained from a spin-unrestricted Kohn−Sham (UKS) calculation for the S = 3/2 ground state of $[Co^{III}(AP^{\bullet})_3]^0$ (Figure 13) yielded the expected electronic structure containing

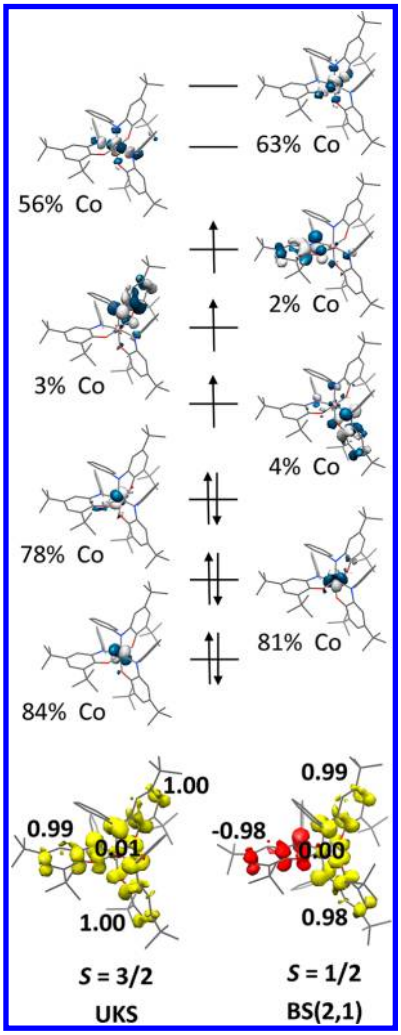

Figure 13. Qualitative FMO diagram for S = 3/2 $[Co^{III}(AP^{\bullet})_3]^0$ and spin density plots (yellow: α-spin; red: β-spin), plus Mulliken spin density populations, obtained from DFT calculation of the S = 3/2 and S = 1/2 spin states.

three filled metal-centered molecular orbitals (MOs) each of ~80% Co character (i.e., a low-spin Co^{III} d^6 ion) and three ligand-centered singly occupied molecular orbitals (SOMOs). Not only is the geometry optimized structure in excellent agreement with the X-ray structure (Chart 2), the geometries of S = 3/2 and 1/2 ground and excited states are identical. The UKS calculation for the S = 1/2 excited state converged to a BS(2,1) solution in which a through-space ligand radical−radical coupling was observed (Figure S8, Supporting Information). A calculation performed using the BS(2,1) formalism and the corresponding geometry optimized structure yielded a ferromagnetic coupling constant via the Yamaguchi

dx.doi.org/10.1021/ic302743s | Inorg. Chem. 2013, 52, 4472−4487

Chart 2. Experimental[34] and Calculated Bond Distances of $[Co^{III}(AP^{\bullet})_3]^0$ (S = 3/2)

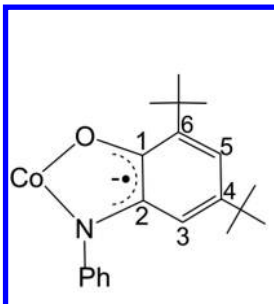

	exp.(av.)	Calcd.
Co-O	1.888(1)	1.912
Co-N	1.934(1)	1.972
O-C1	1.304(2)	1.297
N-C2	1.347(2)	1.344
C1-C2	1.438(2)	1.452
C2-C3	1.428(2)	1.426
C3-C4	1.369(2)	1.382
C4-C5	1.433(2)	1.433
C5-C6	1.380(2)	1.388
C6-C1	1.427(2)	1.437

approach (eq 8) of J_{calcd} = +29 cm^{-1}, which is in excellent agreement with the experimentally determined value. (The meaning of the energies E_{HS} and E_{BS} and spin expectation values $<S^2>$ are described in ref 35.) Using the X-ray structure, a J_{calcd}-value of +56 cm^{-1} was obtained. On the basis of these calculations, we can conclude that the complex electronic structure of such ligand radical-containing complexes is adequately and reliably described by the DFT protocol used here.

$$J = \frac{E_{HS} - E_{BS}}{\langle S^2\rangle_{HS} - \langle S^2\rangle_{BS}} \quad (8)$$

The electronic structure of the analogous Cr^{III} complex **5** provides an interesting contrast to $[Co^{III}(AP^{\bullet})_3]^0$ because the metal center in the former has three unpaired electrons in addition to the three unpaired electrons located on the three $(CF_3AP^{\bullet})^{1-}$ ligands. These spins antiferromagnetically couple to one another to yield the observed singlet ground state. In agreement with this electronic description, the geometry optimized structure from the BS(3,3) calculation was found to be 47 kcal mol^{-1} lower in energy than the spin-restricted Kohn-Shan (RKS) solution. (Note, the RKS solution corresponds to a closed-shell electronic structure, as would be expected for Cr^0.) Other than the Cr−O and Cr−N distances being slightly overestimated, the structural parameters of the BS(3,3) geometry optimized structure are in excellent agreement with the crystal structure. Figure 14 shows a qualitative FMO and a Mulliken spin density plot of the molecule. The SOMOs of the three equivalent $(CF_3AP^{\bullet})^{1-}$ ligands (<8% Cr character) couple antiferromagnetically with the three singly occupied metal d orbitals (~90% Cr character), which correspond to the t_{2g} set in O_h symmetry. Additionally, two virtual orbitals with 75% Cr character can be identified, which correspond to the e_g set in O_h symmetry. The calculated antiferromagnetic coupling is very strong (J_{calcd} = −683 cm^{-1}), so it cannot be experimentally verified in the temperature range of 2−300 K.

A very similar result has been obtained for **4**, where three α-diiminate radical monoanions are coordinated to a Cr^{III} ion and the BS(3,3) solution of the geometry optimized structure is 41 kcal mol^{-1} lower in energy than the RKS case. Once again, the calculated bond lengths of the π-radical anions agree very well with the experimental values; and three metal-centered (>90% Cr character) and three ligand-centered (<10% Cr character) SOMOs can be identified (Figures S5 and S11, Supporting Information), which strongly antiferromagnetically couple to one another to yield a J_{calcd} of −700 cm^{-1} and the observed singlet ground state.

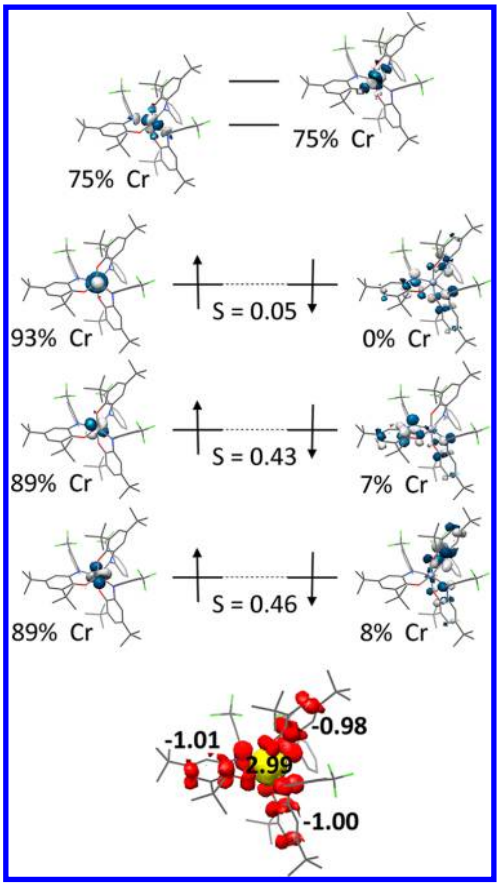

Figure 14. Qualitative FMO diagram for S = 0 $[Cr^{III}(CF_3AP^{\bullet})_3]^0$ (**5**) and spin density plot (yellow: α-spin; red: β-spin), plus Mulliken spin density populations, obtained from a BS(3,3) DFT calculation.

Next, the calculated electronic structures of the four members of the electron transfer series $[Cr(PDI)_2]^{3+/2+/1+/0}$ are described, starting with the most oxidized member. As expected, the trication possesses an S = 3/2 ground state derived from three Cr-centered SOMOs (t_{2g} in O_h symmetry) and the electronic structure $[Cr^{III}(PDI^0)_2]^{3+}$ (Figure S12, Supporting Information). This is reflected in the Mulliken spin density population analysis (Figure S6, Supporting Information), which places 3.23 unpaired electrons on the Cr^{III} center and very little spin density on the ligands (approximately −0.11 spins on each). Consistent with this picture, the geometry optimized structure contains two equivalent neutral (PDI^0) ligands (Scheme 1) whose C−C and C−N bond distances are in excellent agreement with those reported for the crystal structures of $[M^{II}(PDI^0)_2]^{2+}$ (M = Mn^{II}, Fe^{II}, Co^{II}, Cu^{II}, and Zn^{II}).[31]

UKS calculations for the S = 1 dication **6** underwent spontaneous symmetry breaking to yield a BS(3,1) solution. Interestingly, in both the geometry optimized and X-ray structures, the two PDI ligands were found to be inequivalent. Whereas one has C−C and C−N bond lengths typical of a neutral (PDI^0) ligand, the corresponding bond distances in the other are characteristic of a $(PDI^{\bullet})^{1-}$ π-radical anion. Indeed, its qualitative FMO diagram (Figure 15) contains three metal-centered SOMOs (i.e., Cr^{III}) and a ligand-centered SOMO, which strongly antiferromagnetically couple to one another (J_{calcd} = −1200 cm^{-1}) to give the electronic structure

dx.doi.org/10.1021/ic302743s | Inorg. Chem. 2013, 52, 4472−4487

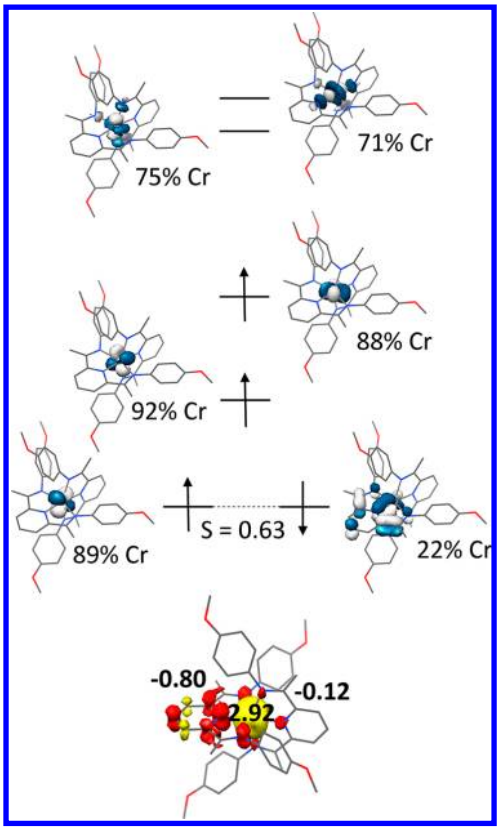

Figure 15. Qualitative FMO diagram for $S = 1$ $[Cr^{III}(PDI^0)(PDI^\bullet)]^{2+}$ (**6**) and spin density plot (yellow: α-spin; red: β-spin), plus Mulliken spin density populations, obtained from a BS(3,1) DFT calculation.

description $[Cr^{III}(PDI^0)(PDI^\bullet)]^{2+}$ ($S = 1$). This is reflected in the Mulliken spin density population analysis, which places 2.92 α-spins on the central Cr^{III} ion, 0.80 β-spins on one ligand, and only 0.12 β-spins on the other. This description is analogous to that previously reported for the dication $[Cr^{III}(terpy^0)(terpy^\bullet)]^{2+}$ ($S = 1$).[3d]

Similarly, UKS calculations for $S = 1/2$ $[Cr(PDI)_2]^{1+}$ undergo spontaneous symmetry breaking to yield BS(3,2) solutions. In this case, both PDI ligands were found to be equivalent with C−C and C−N bond distances typical of $(PDI^\bullet)^{1-}$. The electronic structure is therefore best described as $[Cr^{III}(PDI^\bullet)_2]^{1+}$, wherein the two ligand radicals strongly antiferromagnetically couple to a Cr^{III} ion to yield the $S = 1/2$ ground state ($J_{calcd} = -1052$ cm^{-1}). The qualitative FMO diagram and the Mulliken spin density population analysis confirm this notion (Figures S13 and S6, Supporting Information).

Calculations for the neutral complex $[Cr(PDI)_2]^0$ ($S = 0$) yield a BS(3,3) ground state and clearly shows that this species also contains a Cr^{III} ion. The two PDI ligands were found to be equivalent with C−C and C−N bond lengths intermediate between those of a $(PDI^\bullet)^{1-}$ radical anion and those of a $(PDI^{\bullet\bullet})^{2-}$ dianion, which has been calculated to have a $S = 1$ ground state.[32] Indeed, the average of typical $N_{imine}-C_{imine}$, $C_{imine}-C_{ipso}$, and $C_{ipso}-N_{pyridine}$ bond lengths (Scheme 1) for a $(PDI^\bullet)^{1-}$ and a $(PDI^{\bullet\bullet})^{2-}$ at 1.341, 1.456, and 1.378 Å, respectively, is in very close agreement with the values of 1.336, 1.437, and 1.373 Å calculated for $[Cr(PDI)_2]^0$. Thus, there are three unpaired electrons delocalized over two PDI ligands, which couple antiferromagnetically to the three metal-centered electrons affording a singlet ground state ($J_{calcd} = -1000$ cm^{-1}). The electronic structure is therefore best described as $[Cr^{III}(PDI^\bullet)(PDI^{\bullet\bullet})]^0$, which is reflected in the FMO diagram and Mulliken spin density population analysis (Figures S14 and S7, Supporting Information).

As observed in its X-ray structure, the two acetate ligands in the UKS optimized geometry of the $S = 3/2$ monocationic complex **3** coordinate *cis* with respect to one another. Both bpy ligands were found to be equivalent and have structural parameters in excellent agreement with those in uncoordinated (bpy^0)[5a] and the complex $[Cr^0(CO)_4(bpy^0)]^0$.[36] Thus, like *cis*-$[Cr^{III}(bpy^0)_2Cl_2]^{1+}$,[28] **3** is a Werner-type octahedral Cr^{III} species, so it has the electronic structure $[Cr^{III}(bpy^0)_2(CH_3CO_2)_2]^{1+}$ (see FMO Figure S9, Supporting Information).

Addition of an electron to monocationic **3** yields the $S = 1$ neutral species **1**. The two bpy ligands in the geometry optimized structure of **1** were found to be equivalent, but their C−C and C−N bond distances suggest an oxidation level intermediate between (bpy^0) and $(bpy^\bullet)^{1-}$. Hence, one unpaired electron is delocalized over both bpy ligands and reduction is ligand centered. This is in contrast to the crystal structure of $[Cr^{III}(^tbpy^0)(^tbpy^\bullet)Cl_2]^0$ ($S = 1$),[3f] where the corresponding electron is localized on a single bpy ligand. Application of the conductor-like screening model (COSMO)[37] to model solvation in water has been shown to cause spin localization in several instances[3b,f] but was found to have no effect in the case of **1**. However, the experimental data (especially the broad LLIVCT band at ~4000 cm^{-1} shown in Figure 2) suggest that **1**, at least in the solid state, possesses localized (bpy^0) and $(bpy^\bullet)^{1-}$ ligands (class I or II). Regardless, the electronic structure of **1** is best described as $[Cr^{III}(bpy^0)(bpy^\bullet)(CH_3CO_2)_2]^0$, with the $S = 1$ ground state being obtained via antiferromagnetic coupling ($J_{calcd} = -989$ cm^{-1}) between the Cr^{III} center and unpaired spin of the $(bpy^\bullet)^{1-}$ ligand (see the qualitative FMO diagram and Mulliken spin density population analysis in Figures S10 and S4, Supporting Information). It most certainly does not contain low-spin Cr^{II}, as suggested in the original reports.[5,6]

Finally, UKS calculations for neutral complex **2** ($S = 1$) converged exclusively to BS(3,1) solutions. The corresponding optimized geometry displayed excellent agreement with experiment, so contains a *N*,*N*′-coordinated bpy ligand that is clearly a π-radical anion. Like in **1**, the $S = 1$ ground state is attained by strong antiferromagnetic coupling ($J_{calcd} = -592$ cm^{-1}) of the unpaired electron on the $(bpy^\bullet)^{1-}$ ligand with one of the three unpaired electrons at the t_{2g}^3 Cr^{III} center (see FMO scheme in Figure 16). The above picture is reflected in the Mulliken spin density population analysis, which displays 3.11 α-spin on the chromium center, 1.00 β-spin on the bpy ligand, and virtually no spin density on the acetate and isopropylamine ligands. Once again, no evidence was found for a low-spin Cr^{II} formulation,[5,6] so the electronic structure of **2** is $[Cr^{III}(bpy^\bullet)(CH_3CO_2)_2(^iPrNH_2)_2]^0$.

DISCUSSION

In this study, the homoleptic complexes **4**, **5**, and **7** have been shown by X-ray crystallography to contain three equivalent $S = 1/2$ π-radical anions produced by one e^- reduction of α-diimine, *ortho*-iminoquinone, and bpy ligands, respectively. This has also been previously demonstrated to be the case for neutral complexes containing 2,2′-bipyridine radical anions,[3b] *ortho*-semiquinonate,[8b,38] and 1,2-dithiolene derived π-radical anions.[10b] In all of these complexes, the energies of the Cr K-

dx.doi.org/10.1021/ic302743s | Inorg. Chem. 2013, 52, 4472−4487

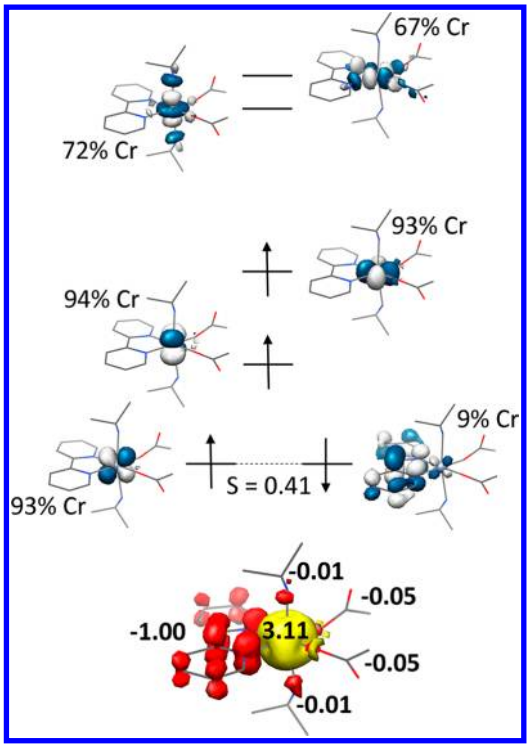

Figure 16. Qualitative FMO diagram for $S = 1$ $[Cr^{III}(bpy^{\bullet})(CH_3CO_2)_2(^{i}PrNH_2)_2]^0$ (**2**) and spin density plot (yellow: α-spin; red: β-spin), plus Mulliken spin density populations, obtained from a BS(3,1) DFT calculation.

pre-edge (5990.4 ± 0.4 eV) and the rising edge confirm the presence of Cr^{III}. Furthermore, their electronic spectra are dominated by intense ($\varepsilon > 1000$ $M^{-1}cm^{-1}$) absorption bands in the visible and NIR region that cannot be assigned as d → d transitions of a 6-coordinate Cr^{III} ion, but instead correspond to intraligand $\pi \rightarrow \pi^*$ transitions. Additionally, DFT calculations for all of these species converge to BS(3,3) ground states, whose geometry optimized structures display structural parameters in excellent agreement with X-ray crystallographic data. In all cases, Mulliken spin density population and FMO analyses reveals that there are three unpaired electrons on the ligands and three unpaired electrons at the t_{2g}^3 Cr^{III} center. These unpaired spins couple strongly in an antiferromagnetic fashion ($J = -400$ to -800 cm^{-1}) to afford the experimentally observed singlet ground states.

The second group of compounds, encompassing $[Cr^{III}(PDI^0)(PDI^{\bullet})]^{2+}$ **6** and $[Cr^{III}(terpy^0)(terpy^{\bullet})]^{2+}$,[3d] are dicationic $S = 1$ species for which high resolution X-ray crystallography unambiguously shows that one tridentate ligand is neutral and the other is a π-radical anion. This ligand-centered unpaired electron, in either $(terpy^{\bullet})^{1-}$ or $(PDI^{\bullet})^{1-}$, couples strongly in an antiferromagnetic fashion to one of three unpaired electrons on the Cr^{III} center to give the observed triplet ground state. The electronic spectra of these complexes are once again dominated by intramolecular $\pi \rightarrow \pi^*$ and $\pi^* \rightarrow \pi^*$ transitions characteristic of π-radical anions. In addition, both complexes exhibit a broad LLIVCT band, which appears at ~4500 cm^{-1} for **6** (observed) and at ~1900 cm^{-1} for $[Cr^{III}(terpy^0)(terpy^{\bullet})]^{2+}$ (calculated, not observed). Thus, these complexes irrefutably contain Cr^{III}, and their electronic structure should *not* be described as $[Cr^{II}(terpy^0)_2]^{2+}$ and $[Cr^{II}(PDI^0)_2]^{2+}$.

Reaction between the dimer $[Cr^{II}_2(\mu\text{-}CH_3CO_2)_4]^0$ and (bpy^0) in THF produces the mononuclear complex **1** containing two *N,N′*-coordinated bpy ligands and two *cis*-oriented monodentate acetate ligands, as was suggested by the original authors and now are unequivocally established by X-ray crystallography. In contrast to the notion that **1** is a low-spin Cr^{II} species ($S = 1$), we have demonstrated that it contains a $(bpy^{\bullet})^{1-}$ π-radical anion and, using Cr K-edge XAS, a Cr^{III} ion. Accordingly, the electronic structure for **1** is best described as $[Cr^{III}(bpy^0)(bpy^{\bullet})(CH_3CO_2)_2]^0$, wherein the $S = 1$ ground state is obtained by strong antiferromagnetic coupling of the unpaired electron on the $(bpy^{\bullet})^{1-}$ ligand with the $S = 3/2$ Cr^{III} center. We previously found a similar electronic structure for $[Cr^{III}(^{t}bpy^0)(^{t}bpy^{\bullet})Cl_2]^0$ ($S = 1$)[3f] in which the two ^{t}bpy ligands were readily identified by X-ray crystallography as having different redox states, with one being neutral and the other a monoanionic π-radical anion, making this a class I (fully localized) system. The situation is not so straightforward for **1** because, although the two bpy ligands are equivalent (related by crystallographic C_2 symmetry), this could either be the result of a static disorder or due to class II/III (delocalized) behavior. DFT calculation of geometry optimized structures for **1** using the BS(3,1) formalism in both the gas phase *and* using the COSMO solvent model converged to the same delocalized electronic structure. However, this may be a consequence of the known bias of DFT methodologies toward delocalization of charge. As a consequence, we are unable to establish whether **1** is truly a class II/III system or not.

Interestingly, isopropylamine and other monodentate primary amines are able to displace one of the two bpy ligands in **1** to yield $[Cr^{III}(bpy^{\bullet})(^{i}PrNH_2)_2(CH_3CO_2)_2]^0$ (**2**). It appears that the more weakly bound neutral (bpy^0) ligand in **1** is replaced, whereas the more strongly bound $(bpy^{\bullet})^{1-}$ remains coordinated. In the structure of $[Cr^{III}(^{t}bpy^0)_2(^{t}bpy^{\bullet})](PF_6)_2$, we have shown that the average Cr−N distance of the $Cr(^{t}bpy^0)$ chelates are longer (weaker) at 2.06 Å and shorter (stronger) in the $Cr^{III}(^{t}bpy^{\bullet})$ chelate at 1.99 Å. This supports the above reactivity postulate and, indirectly, the notion that the $Cr(bpy^0)$ and $Cr(bpy^{\bullet})$ chelates are localized in **1**. It is important to note that neither **1** nor **2** can be described as a low-spin Cr^{II} species. Finally, one-electron oxidation of **1** yields the Werner type complex *cis*-$[Cr^{III}(bpy^0)_2(CH_3CO_2)_2]^{1+}$ (**3**), whose UV−vis and Cr K-edge XAS spectra are indicative of a Cr^{III} ion. Hence, oxidation of **1** to **3** is a ligand-centered process.

Overall, this study augments a general picture that we and others have built over the years which indicates that Cr complexes of potentially redox noninnocent ligands in which the Cr ion possesses a formal oxidation state of ≤ +II almost invariably possess a highly stable high-spin d^3 electronic configuration at the Cr center. There are exceptions, which are associated with strongly π-accepting ancillary ligands[36] and geometries that stabilize alternate electron configurations.[4] However, in the majority of 6-coordinate complexes of this type, it can be fairly safely assumed that redox events are ligand centered, which renders formal oxidation state assignment a ligand-centric consideration. Electronic ground states can then be reliably predicted using the Goodenough-Kanamori rules.[39]

■ ASSOCIATED CONTENT

Ⓢ Supporting Information

Crystallographic information files (cif) for **1**−**7**, SQUID data, cyclic voltammetry for **5**, and further information regarding the

dx.doi.org/10.1021/ic302743s | Inorg. Chem. 2013, 52, 4472−4487

DFT calculations, including tables of atomic coordinates, bond distances, and energies, plus additional Mulliken spin density plots and qualitative frontier molecular orbital diagrams. This material is available free of charge via the Internet at http://pubs.acs.org.

AUTHOR INFORMATION

Corresponding Author

*E-mail: karl.wieghardt@cec.mpg.de.

Author Contributions

[¶]M.W. and J.E. contributed equally.

Notes

The authors declare no competing financial interest.

ACKNOWLEDGMENTS

M.W. and J.E. thank the Max Planck Society for financial support and Ms. Heike Schucht and Mr. Andreas Göbels for technical assistance. S.D. acknowledges funding from the Max Planck Society, Cornell University, and the Alfred P. Sloan Foundation. Portions of this research were based upon work supported by the National Science Foundation under Grant No. CHE-0911081 awarded to K.H.T. Other components were carried out at the Stanford Synchrotron Radiation Lightsource, a Directorate of SLAC National Accelerator Laboratory, and an Office of Science User Facility operated for the U.S. Department of Energy Office of Science by Stanford University.

REFERENCES

(1) Forum Issue on Redox-Active Ligands , *Inorg. Chem.* **2011**, *50*, 9737.

(2) Chaudhuri, P.; Verani, C. N.; Bill, E.; Bothe, E.; Weyhermüller, T.; Wieghardt, K. *J. Am. Chem. Soc.* **2001**, *123*, 2213.

(3) (a) Scarborough, C. C.; Wieghardt, K. *Inorg. Chem.* **2011**, *50*, 9773. (b) Scarborough, C. C.; Sproules, S.; Weyhermüller, T.; DeBeer, S.; Wieghardt, K. *Inorg. Chem.* **2011**, *50*, 12446. (c) Bowman, A. C.; Sproules, S.; Wieghardt, K. *Inorg. Chem.* **2012**, *51*, 3707. (d) Scarborough, C. C.; Lancaster, K. M.; DeBeer, S.; Weyhermüller, T.; Sproules, S.; Wieghardt, K. *Inorg. Chem.* **2012**, *51*, 3718. (e) England, J.; Scarborough, C. C.; Weyhermüller, T.; Sproules, S.; Wieghardt, K. *Eur. J. Inorg. Chem.* **2012**, 4605. (f) Scarborough, C. C.; Sproules, S.; Doonan, C. J.; Hagen, K. S.; Weyhermüller, T.; Wieghardt, K. *Inorg. Chem.* **2012**, *51*, 6969.

(4) Irwin, M.; Doyle, L. R.; Krämer, T.; Herchel, R.; McGrady, J. E.; Goicoechea, J. M. *Inorg. Chem.* **2012**, *51*, 12301.

(5) Herzog, S.; Oberender, H.; Pahl, S. *Z. Chem.* **1963**, *3*, 102.

(6) Herzog, S.; Oberender, H.; Pahl, S. *Z. Naturforsch.* **1963**, *18b*, 158.

(7) Note that throughout this paper we use the abbreviation (bpy) in a generic sense without specifying the oxidation level of this ligand. If the latter is intended, we use (bpy^0) for the neutral ligand, $(bpy^{\bullet})^{1-}$ for the π-radical anion, and $(bpy^{2-})^{2-}$ for the diamagnetic dianion. Crystal structures of "uncoordinated" (bpy^0), $(bpy^{\bullet})^{1-}$, and $(bpy^{2-})^{2-}$ have been reported. (a) (bpy^0): Chisholm, M. H.; Huffman, J. C.; Rothwell, I. P.; Bradley, P. G.; Kress, N.; Woofdruff, W. M. *J. Am. Chem. Soc.* **1981**, *103*, 4945. (b) $(bpy^{\bullet})^{1-}$: Gore-Randall, E.; Irwin, M.; Denning, M. S.; Giocoechea, J. M. *Inorg.Chem.* **2009**, *48*, 8304. (c) $(bpy^{2-})^{2-}$: Bock, H.; Lehn, J.-M.; Pauls, J.; Holl, S.; Krenzel, V. *Angew. Chem., Int. Ed.* **1999**, *38*, 952.

(8) (a) Benelli, C.; Dei, A.; Gatteschi, D.; Güdel, H.; Pardi, L. *Inorg. Chem.* **1989**, *28*, 3089. (b) Kapre, R. R.; Bothe, E.; Weyhermüller, T.; DeBeer, S.; Muresan, N.; Wieghardt, K. *Inorg. Chem.* **2007**, *46*, 7827.

(9) Spikes, G. H.; Sproules, S.; Bill, E.; Weyhermüller, T.; Wieghardt, K. *Inorg. Chem.* **2008**, *47*, 10935.

(10) (a) Sproules, S.; Wieghardt, K. *Coord. Chem. Rev.* **2011**, *255*, 837. (b) Banerjee, P.; Sproules, S.; Weyhermüller, T.; DeBeer George, S.; Wieghardt, K. *Inorg. Chem.* **2009**, *48*, 5829.

(11) Kliegman, J. M.; Barnes, R. K. *Tetrahedron* **1970**, *26*, 2555.

(12) Bill, E.; Bothe, E.; Chaudhuri, P.; Chlopek, K.; Herebian, D.; Kokatam, S.; Ray, K.; Weyhermüller, T.; Neese, F.; Wieghardt, K. *Chem.—Eur. J.* **2005**, *11*, 204.

(13) Aleya, E. C.; Merrell, P. H. *Synth. React. Inorg. Met.−Org. Chem.* **1974**, *4*, 535.

(14) Chun, H.; Verani, C. N.; Chaudhuri, P.; Bothe, E.; Bill, E.; Weyhermüller, T.; Wieghardt, K. *Inorg.Chem.* **2001**, *40*, 4157.

(15) Bain, G. A.; Berry, J. F. *J. Chem. Educ.* **2008**, *85*, 532.

(16) (a) George, G. N. EXAFSPAK; Stanford Synchroton Radiation Laboratory, Stanford Linear Accelerator, Stanford University: Stanford, CA, 2000. (b) Delgado-Jaime, M. U.; Mewis, C. P.; Kennepohl, P. *J. Synchrotron Radiat.* **2010**, *17*, 132.

(17) (a) Sheldrick, G. M. SADABS, Bruker-Siemens Area Detector Absorption and Other Corrections, University of Göttingen, Germany, 2006; Version 2008/1. (b) ShelTXL 6.14; Bruker AXS Inc.: Madison, WI, USA, 2003. (c) Sheldrick, G. M. ShelXL97, University of Göttingen, Germany, 1997.

(18) Neese, F. Orca an Ab Initio, Density Functional and Semiempirical Electronic Structure Program Package, version 2.8; Universität Bonn: Bonn, Germany, 2011.

(19) (a) Becke, A. D. *Phys. Rev. A* **1988**, *38*, 3098. (b) Becke, A. D. *J. Chem. Phys.* **1993**, *98*, 5648. (c) Lee, C. T.; Yang, W. T.; Parr, R. G. *Phys. Rev. B* **1988**, *37*, 785.

(20) (a) Weigend, F.; Ahlrichs, R. *Phys. Chem. Chem. Phys.* **2005**, *7*, 3297. (b) Schäfer, A.; Huber, C.; Ahlrichs, R. *J. Chem. Phys.* **1994**, *100*, 5829.

(21) (a) Eichkorn, K.; Weigend, F.; Treutler, O.; Ahlrichs, R. *Theor. Chem. Acc.* **1997**, *97*, 119. (b) Eichkorn, K.; Treutler, O.; Öhm, H.; Häser, M.; Ahlrichs, R. *Chem. Phys. Lett.* **1995**, *240*, 283. (c) Eichkorn, K.; Treutler, O.; Öhm, H.; Häser, M.; Ahlrichs, R. *Chem. Phys. Lett.* **1995**, *242*, 652.

(22) (a) Neese, F.; Wennmohs, F.; Hansen, A.; Becker, U. *Chem. Phys.* **2009**, *356*, 98. (b) Kossmann, S.; Neese, F. *Chem. Phys. Lett.* **2009**, *481*, 240. (c) Neese, F. *J. Comput. Chem.* **2003**, *24*, 1714.

(23) (a) Noodleman, L. *J. Chem. Phys.* **1981**, *74*, 5737. (b) Noodleman, L.; Norman, J. G.; Osborne, J. H.; Aizman, A.; Case, D. A. *J. Am. Chem. Soc.* **1985**, *107*, 3418. (c) Noodleman, L.; Davidson, E. R. *Chem. Phys.* **1986**, *109*, 131. (d) Noodleman, L.; Case, D. A.; Aizman, A. *J. Am. Chem. Soc.* **1988**, *110*, 1001. (e) Noodleman, L.; Peng, C. Y.; Case, D. A.; Monesca, J. M. *Coord. Chem. Rev.* **1995**, *144*, 199.

(24) Neese, F. *J. Phys. Chem. Solids* **2004**, *65*, 781.

(25) Pettersen, E. F.; Goddard, T. D.; Huang, C. C.; Couch, G. S.; Greenblatt, D. M.; Meng, E. C.; Ferrin, T. E. *J. Comput. Chem.* **2004**, *25*, 1605−1612.

(26) Neese, F. *Inorg. Chim. Acta* **2002**, *337*, 181.

(27) (a) DeBeer George, S.; Petrenko, T.; Neese, F. *Inorg. Chim. Acta* **2008**, *361*, 965. (b) DeBeer George, S.; Petrenko, T.; Neese, F. *J. Phys. Chem. A.* **2008**, *112*, 12936.

(28) Kar, T.; Liao, M.-S.; Biswas, S.; Sarkar, S.; Dey, K.; Yap, G. P. A.; Kreisel, K. *Spectrochim. Act. Part* **2006**, *A65*, 882.

(29) (a) Ghosh, M.; Sproules, S.; Weyhermüller, T.; Wieghardt, K. *Inorg. Chem.* **2008**, *47*, 5963. (b) Kreisel, K. A.; Yap, G. P. A.; Dmitrenko, O.; Landis, C. R.; Theopold, K. H. *J. Am. Chem. Soc.* **2007**, *129*, 14162. (c) Kreisel, K. A.; Yap, G. P. A.; Theopold, K. H. *Inorg. Chem.* **2008**, *47*, 5293.

(30) Carter, S. M.; Sia, A.; Shaw, M. J.; Heyduk, A. F. *J. Am. Chem. Soc.* **2008**, *130*, 5838.

(31) de Bruin, B.; Bill, E.; Bothe, E.; Weyhermüller, T.; Wieghardt, K. *Inorg. Chem.* **2000**, *39*, 2936.

(32) Bart, S. C.; Chlopek, K.; Bill, E.; Bouwkamp, M. W.; Lobkovsky, E.; Neese, F.; Wieghardt, K.; Chirik, P. *J. Am. Chem. Soc.* **2006**, *128*, 13901.

(33) Banerjee, P.; Sproules, S.; Weyhermüller, T.; DeBeer George, S.; Wieghardt, K. *Inorg. Chem.* **2009**, *48*, 5829.

(34) Verani, C. N.; Gallert, S.; Bill, E.; Weyhermüller, T.; Wieghardt, K.; Chaudhuri, P. *Chem. Commun.* **1999**, 1747.
(35) (a) Soda, T.; Kitagawa, Y.; Onishi, T.; Takano, Y.; Shigeta, Y.; Nagao, H.; Yoshioka, Y.; Yamaguchi, K. *Chem. Phys. Lett.* **2000**, *319*, 223. (b) Yamaguchi, K.; Takahara, Y.; Fueno, T. In *Applied Quantum Chemistry*; Smith, V. H., Ed.; Reidel: Dordrecht, the Netherlands, 1986; p 155.
(36) Le Floch, P.; Carmichael, D.; Ricard, L.; Mathey, F.; Jutand, A.; Amatore, C. *Organometallics* **1992**, *11*, 2475.
(37) Klamt, A.; Jonas, V.; Burger, T.; Lohrenz, J. C. W. *J. Phys. Chem. A* **1998**, *102*, 5074.
(38) Pierpont, C. G. *Coord. Chem. Rev.* **2001**, *219*−*221*, 415.
(39) Kahn, O. *Molecular Magnetism*; Wiley-VCH Inc.: Weinheim, 1993.